Volcanic, tectonic and mass-wasting processes offshore Terceira Island (Azores) revealed by high-resolution seafloor mapping.

Volcanic, tectonic and mass-wasting processes offshore Terceira Island (Azores) revealed by high-resolution seafloor mapping

D. Casalbore · C. Romagnoli · A. Pimentel · R. Quartau · D. Casas · G. Ercilla · A. Hipólito · A. Sposato · F. L. Chiocci

Abstract Terceira Island, in the Azores Archipelago, lies at the intersection of four submarine volcanic ridges. New high-resolution bathymetric and seismic reflection data have been used to analyze the main volcanic, tectonic and mass-wasting features of the island offshore. Volcanic features such as linear volcanic centers, and pointy and flat-topped cones are mainly concentrated on the narrow western and north-western ridges, characterized by an overall rugged morphology. Fault scarps dominate mainly the broad eastern and south-eastern ridges, which are characterized by an overall smooth and terrace-like morphology. On the eastern ridge, faults form a series of horsts and grabens related to the onshore Lajes Graben. The strikes of the fault scarps, linear volcanic centers and alignment of volcanic cones on the ridges reveal two main structural trends, WNW–ESE and NNW–SSE, consistent with the main tectonic structures observed on the Azores Plateau. In contrast, a large variability of strike was observed in inter-ridge areas, reflecting the relative importance of regional and local stresses in producing these structures. Mass-wasting features are subordinate and mostly represented by hundred meter-wide scars that indent the edge of the insular shelf surrounding the island, apart from two large, deeper scars identified on the southern steep flank of the western ridge. Finally, the remarkable morpho-structural differences between the western and eastern ridges are discussed in the framework of the evolution

Editorial responsibility: A. Gudmundsson

Electronic supplementary material The online version of this article (doi:10.1007/s00445 015 0905 3) contains supplementary material, which is available to authorized users.

D. Casalbore (✉) · A. Sposato · F. L. Chiocci
Istituto di Geologia Ambientale e Geoingegneria (Consiglio Nazionale delle Ricerche), Area della Ricerca di Roma 1, Montelibretti, Via Salaria Km 29,300, Monterotondo, Roma, Italy
e mail: daniele.casalbore@igag.cnr.it

C. Romagnoli
Dipartimento di Scienze Biologiche, Geologiche ed Ambientali, Università di Bologna, P.za Porta S. Donato 1, 40126 Bologna, Italy

A. Pimentel
Centro de Informação e Vigilância Sismovulcânica dos Açores, 9501 801 Ponta Delgada, Azores, Portugal

A. Pimentel · A. Hipólito
Centro de Vulcanologia e Avaliação de Riscos Geológicos, University of the Azores, 9501 801 Ponta Delgada, Azores, Portugal

R. Quartau
Divisão de Geologia Marinha e Georecursos, Instituto Português do Mar e da Atmosfera I.P., Rua C do Aeroporto, 1749 077 Lisboa, Portugal

R. Quartau
Instituto Dom Luiz, Faculdade de Ciências da Universidade de Lisboa, Campo Grande, Edifício C8, Piso 3, 1749 016 Lisboa, Portugal

D. Casas
Geological Survey of Spain, Madrid, Spain

G. Ercilla
Departamento de Geología Marina Instituto de Ciencias del Mar CMIMA CSIC, Barcelona, Spain

F. L. Chiocci
Dipartimento Scienze della Terra, Sapienza Università di Roma, Roma, Italy

of the Terceira volcanic edifice and hypothesized to reflect successive stages of ridge evolution.

Keywords Multibeam bathymetry · Morphometry · Submarine volcanism · Volcanic ridges · Tectonic control · Terceira Rift

Introduction

The Azores Archipelago is located near the triple junction between the Eurasian, Nubian, and North-American plates (EU, NU, and NA in Fig. 1, lower-left inset). The nature of the northern and southern branches of this triple junction, segments of the Mid-Atlantic Ridge (MAR), is relatively well-known (e.g., Gente et al. 2003), whereas volcano-tectonic interaction and kinematics of the eastern branch, i.e., the Terceira Rift and associated structures are still poorly constrained (e.g., Argus et al. 1989; Calais et al. 2003; Vogt and Jung 2004; Hipólito et al. 2013; Trippanera et al. 2014). Few outcrops and structures related to the earlier stages of development in this region are visible on the islands of the central and eastern groups of Azores due to their very recent volcanism (late Pliocene–Quaternary as indicated by magnetic anomalies, Miranda et al. 1991; Luís and Miranda 2008, and isotopic data, Calvert et al. 2006; Hildenbrand et al. 2008, 2014). Moreover, given that most of the region lies under the sea, a comprehensive understanding of the volcanic and tectonic processes affecting this area relies inevitably on ma-rine studies. The morpho-tectonic setting of the Azores Plateau was reconstructed mostly on the basis of low-resolution bathymetric and side-scan sonar data (e.g., Lourenço et al. 1998), although high-resolution data were lo-cally collected around Pico, Faial, São Jorge, and Terceira (e.g., Ligi et al. 1999; Stretch et al. 2006; Lourenço 2007; Mitchell et al. 2008, 2012a). The plateau is characterized by large-scale linear volcanic ridges, i.e., composite volcanic structures constructed by basaltic fissure volcanism, that

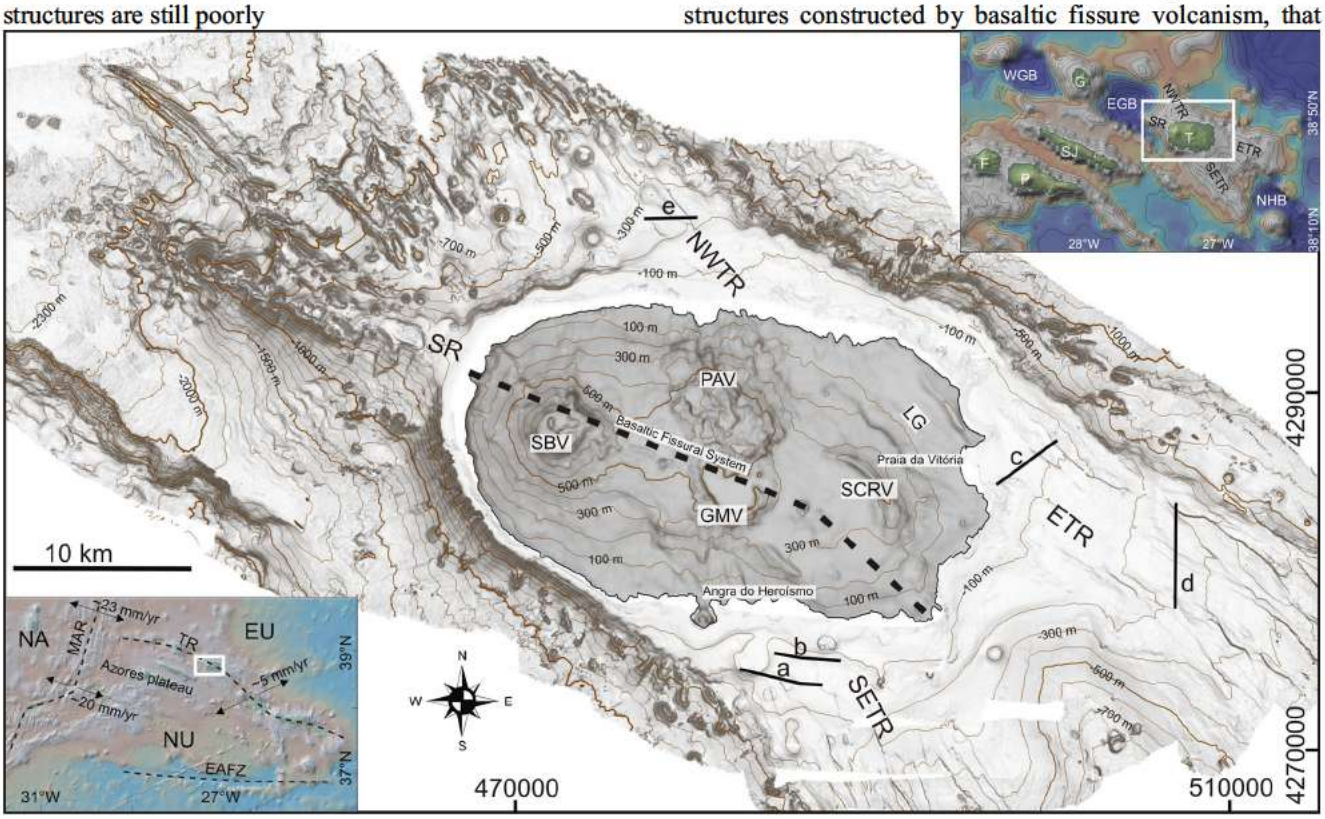

Fig. 1 Shaded relief map with elevation contours every 100 m of Terceira onshore (degraded DTM from topographic maps at the 1:25,000 scale; Instituto Geográfico do Exército 2002a, b, c, d) and offshore (data from Simrad EM 710 and EM122 working at 70 100 and 12 kHz), annotated with the main submarine and subaerial volcanic and tectonic structures (*SR*: Serreta Ridge; *NWTR*: North West Terceira Ridge; *ETR*: East Terceira Ridge; *SETR*: South East Terceira Ridge; *SCRV*: Serra do Cume Ribeirinha Volcano; *PAV*: Pico Alto Volcano; *GMV*: Guilherme Moniz Volcano; *SBV*: Santa Bárbara Volcano; *LG*: Lajes Graben). The *black lines* with the letter *a e* locate the CHIRP profiles shown in Fig. 9. In the *lower left inset*, regional bathymetry of Azores Plateau (data from Ryan et al. 2009), shows the location of the three branches of the Azores Triple Junction (from DeMets et al. 2010).(*MAR*: Mid Atlantic Ridge; *NA*: North American plate; *NU*: Nubian Plate; *EU*: Eurasian plate; *TR*: Terceira Rift; *EAFZ*: East Azores Fracture Zone). *Upper right inset* shows an overview of central Azorean islands, showing the intersection of the four submarine ridges at Terceira; *F*: Faial Island; *P*: Pico Island; *SJ*: São Jorge Island; *G*: Graciosa Island; *T*: Ter ceira Island; *WGB*: Western Graciosa Basin; *EGB*: Eastern Graciosa Ba sin; *NHB*: North Hirondelle Basin

culminate on the subaerial areas (islands), often with central volcanic edifices, and that are flanked by tectonically controlled basins. The large volcanic ridges reflect the regional tectonic pattern of the plateau and represent an important mode of crustal formation (Lourenço et al. 1998). In particular, the Azores region is unique in having numerous active volcanic ridges at a wide range of water depths (Stretch et al. 2006).

The newly collected multibeam bathymetry and seismic reflection profiles (CHIRP) from offshore Terceira Island have enabled us to map and study the main volcanic and tectonic features of these large submarine volcanic ridges (Figs. 1 and 2, see also Chiocci et al. 2013). The aim of the paper is to analyze the spatial distribution and morphometric characteristics of these submarine features in order to gain insights into the growth of the ridges and the related volcano-tectonic processes that interact at local to regional scale. In particular, the emplacement of volcanic cones is fundamental in determining the ridges' development and crust formation (Smith and Cann 1999; Smith et al. 2001). For this reason, their morphometric characteristics have been examined in detail, to assess whether or not they develop self-similarly and if there is any relationship between their shape, water depth, and morpho-structural setting. The variation with depth of edifice type (volcanic cones vs linear eruptive centers) is also discussed. Different stages of formation for the large submarine volcanic ridges are then proposed, based on the marked differences in their size and shape and in the distribution of volcano-tectonic features.

The results obtained are also discussed in the framework of similar studies carried out on other Azorean ridges, such as the Pico Ridge (Stretch et al. 2006; Mitchell et al. 2012a) and Condor Seamount (Tempera et al. 2013), as well as on other volcanic ridges formed in slow-spreading oceanic centers (e.g., Searle et al. 1998; Edwards et al. 2001; Sauter et al. 2002).

Geological setting

The Azores Archipelago consists of nine volcanic islands that emerge from a shallow, triangular-shaped submarine plateau roughly delimited by the 2,000-m isobath: the Azores Plateau (Lourenço et al. 1998). The plateau is thought to result from the complex interaction of rift magmatism associated with a triple junction (Azores Triple Junction) and a deep magmatic anom-aly associated with a hotspot (e.g., Cannat et al. 1999; Gente et al. 2003). This triple junction is formed by a northern branch of the MAR, with a spreading rate of ~23 mm/year, a southern MAR branch with a spreading rate of ~20 mm/year, and a much slower WNW–ESE branch along the Terceira Rift (TR), with a spreading rate of ~5 mm/year (Fig. 1, lower-left inset; DeMets et al. 2010). The latter has been considered a diffuse dextral transtensional zone (e.g., Madeira and Ribeiro 1990; Lourenço et al. 1998; Madeira and Brum da Silveira 2003; Hipólito et al. 2013) accommodating the differential motion between the EU and NU plates due to the higher

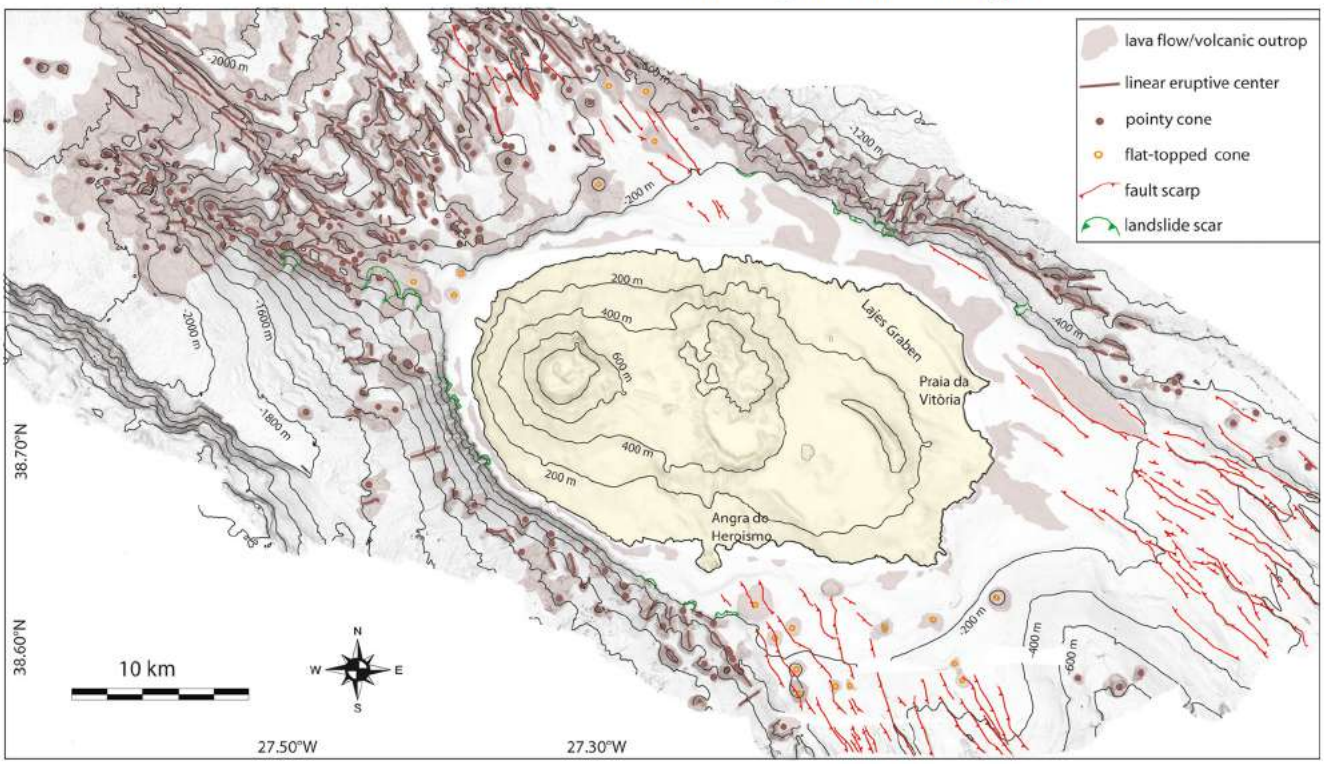

Fig. 2 Morphological map of Terceira offshore, showing the same bathymetry of Fig. 1 and the main recognized volcanic and tectonic structures (modified from Chiocci et al. 2013); see text for details

spreading rate of the northern MAR branch (e.g., Calais et al. 2003; DeMets et al. 2010; Mendes et al. 2013). The geodetic data together with the slightly sinuous axial trace of the TR, its obliqueness (ca. 40°–65°) and seismic source parameters allowed the interpretation as an "ultra-slow" oblique spreading ridge (e.g., Vogt and Jung 2004), similar to the Reykjanes Peninsula (Gudmundsson 1986, 2007). The TR is character-ized by areas of intense volcanism forming giant linear ridges or large central volcanic edifices (islands or seamounts), regu-larly alternating (at ca. 80-km intervals) with fault-controlled rhombic basins (Fig. 1, see also Fig. 4 of Lourenço et al. 1998).

In the Azores region, seismic activity is mainly concentrated along (1) the MAR, (2) the TR (*sensu stricto*, as defined by Machado 1959), and (3) the Faial-Pico and São Jorge Ridges (Fig. 1 upper-right inset; Buforn et al. 1988; Luís et al. 1998; Borges et al. 2007; Dias et al. 2007). Focal mechanisms are varied and suggest a prevalence of WNW–ESE to NW–SE normal and right-lateral oblique faulting, and NNW–SSE left-lateral strike-slip motion (Hirn et al. 1980; Buforn et al. 1988; Lourenço et al. 1998; Silva et al. 2012). The focal mechanisms of the Azores interplate shear zone agree with the structural pattern deduced from neotectonic surveys of the islands (e.g., Madeira and Ribeiro 1990; Madeira and Brum da Silveira 2003; Madeira et al., Active tectonics in the central and eastern Azores Islands along the Eurasia-Nubia boundary: A review, unpublished) indicating the occurrence of alternating transtensile and tensile regimes (e.g., Madeira and Brum da Silveira 2003; Hipólito et al. 2013). However, the processes controlling the structural pattern within the Azorean segment of the EU-NU plate boundary, as well as the dynamics of the stress regime acting there, remain subjects of debate.

Terceira Island is an ideal location to study the volcano-tectonic relationships at local to regional scale, due to its size and position with respect to the TR, as well as its recent seismic and volcanic activity (Miranda et al. 2012). The island comprises four central volcanoes aligned over a WNW–ESE en échelon fault zone that crosses the island, and which is subaerially represented by the Basaltic Fissural System (Fig. 1, hereafter BFS), with alignments of scoria cones and eruptive fissures (Self 1976; Madeira 2005). The oldest edifice is the Serra do Cume–Ribeirinha Volcano (SCRV in Fig. 1; >401 ka, Hildenbrand et al. 2014), which covers the eastern third of the island and is dominated by a large eroded caldera (~7 km wide, the largest caldera in Azores). The Guilherme Moniz and Pico Alto volcanoes (GMV and PAV in Fig. 1, >270 ka and >141 ka, respectively, Calvert et al. 2006; Gertisser et al. 2010) occupy the central part of the island and are superimposed on the SCRV. The GMV culminates with a NW–SE trending elliptic caldera, measuring 4 km by 2 km in diameter; while the PAV is charac-terized by a large pile of thick lava flows and domes that fills a 3.5-km-wide summit caldera. The Santa Bárbara Volcano (SBV in Fig. 1, >65 ka, Hildenbrand et al. 2014) is a conical-shape central edifice that constitutes the western sector of the island. Its summit is truncated by two small overlapping calderas. The SCRV and GMV are considered extinct, while the PAV and SBV are still active and contemporaneous with the BFS (Self 1976; Madeira 2005).

The largest tectonic structure on Terceira is the Lajes Graben in the north-east part of the island (LG in Fig. 1), which is defined by two major NW–SE trending faults, with normal dextral oblique displacement (Madeira 2005). The Lajes Graben faults are estimated to slip at 0.2–0.3 mm/year (Madeira et al., unpublished).

Data and methods

High-resolution multibeam bathymetry and CHIRP seismic reflection profiles (1.7–5.5 kHz) were collected during two oceanographic cruises within the framework of the Eurofleets FAIVI Project (*Features of Azores and Italian Volcanic Islands*) aboard the small launch *Haliotis* and the R/V *L'Atalante* in 2011. Bathymetric data were collected with GeoSwath interferometric sonar operating at 250 kHz in the first −100 m, whereas at greater depths with Simrad EM 710 (70–100 kHz) and EM122(12 kHz) multibeam systems. Data acquisition and processing are described in detail in Chiocci et al. (2013) and Quartau et al. (2014). In this work, marine digital terrain models (DTM's) with cell-sizes varying from 1 to 50 m were produced for water depth less than 100 m and greater than 2,000 m, respectively.

The main morphometric parameters of the submarine volcanic and tectonic features were measured, including their length, basal diameters (maximum/minimum), height, area, slope gradients, and strike of faults and linear volcanic features. Descriptive statistics of the volcanic features are given in Table 1. The parameters of the volcanic cones were measured using the method proposed by Favalli et al. (2009; see Fig. 1 in Supplementary Electronic Material). The average diameter has been computed through the planimetric projection of the cone basal area. The height of the cone has been measured as the elevation difference between the peak and the basal plane of a reconstructed cone fitted via morpho-bathymetric profiles, in order to avoid overestimation in the case of steep basal surfaces. These parameters were used to obtain the aspect ratio (height vs average basal diameter, H/W) of the cone, a morphometric index widely used in subaerial and submarine settings to char-acterize volcanic cones (e.g., Favalli et al. 2009; Mitchell et al. 2012a). Correlations between the morphometric parameters are shown as a Spearman correlation matrix in Table 2.

Results

The seabed around Terceira Island is dominated by four large, elongated volcanic ridges extending several tens of kilometers

Table 1 Descriptive statistics (minimum, maximum, mean, median and standard deviation) of the main morphometric parameters measured for pointy cones, flat-topped cones and linear eruptive centers (LEC)

Pointy cones (108)	Summit depth (m)	Max depth (m)	Height (m)	Max.diameter (m)	Min.diameter (m)	Area (m^2)	Basal diameter (m)	H/W ratio	Min./max.diameters	Average slope gradient (°)		
Min	17	130	28	224	168	35,935	214	0.05	1	8.5		
Max	2,400	2,488	460	3,798	1,773	3,505,208	2,113	0.4	3	37.5		
Mean	805	1,010	123	1,028	712	636,295	847	0.14	1.5	25.3		
Median	522	776	112	925	700	517,661	812	0.14	1.3	26		
St. deviation	647	645	65	503	285	496,865	307	0.05	0.5	5.2		
Flat-topped cones (19)	Summit depth (m)	Max depth (m)	Height (m)	Max.diameter (m)	Min.diameter (m)	Area (m^2)	Basal diameter (m)	H/W ratio	Min./max.diameters	Average slope gradient (°)	Top diameter (m)	Top/basal diameters
Min	12	105	15	730	609	329,349	647	0.02	1	5	300	1.2
Max	215	464	210	3,000	2,000	4,353,614	2,355	0.11	1.8	20	2,500	4.7
Mean	126	243	77	1,504	1,192	1,433,153	1,349	0.06	1.23	14.4	939	2.2
Median	130	240	57	1,300	1,230	1,188,436	1,230	0.05	1.2	14.8	640	1.9
St. deviation	59	110	61	792	448	1,392,294	582	0.03	0.24	4.6	738	1.1
LEC (59)	Summit depth (m)	Max depth (m)	Height (m)	Max.diameter (m)	Min.diameter (m)	Area (m^2)				Average slope gradient (°)		
Min	195	402	13	477	116	60,760				15		
Max	2,375	2,479	225	6,315	926	3,592,868				42.5		
Mean	831	1,057	81	1,472	457	630,327				25.6		
Median	648	954	64	1,180	429	351,684				25		
St. deviation	486	531	46	11,22	195	664,794				5.7		

away from the island (Fig. 1, upper-right inset). In this work, their intermediate and shallow-water parts were surveyed (Fig. 2), while their deeper parts are only recognizable on lower resolution bathymetric maps. The submarine ridges develop off the western sector (Serreta Ridge, SR hereafter), north-western sector (North-West Terceira Ridge, hereafter NWTR), eastern sector (East Terceira Ridge; ETR hereafter), and south-eastern sector (South-East Terceira Ridge; hereafter SETR) of Terceira. The NWTR and SETR are aligned in a NNW–SSE direction, while the SR and ETR mainly trend WNW–ESE. Low-resolution bathymetric data (Fig. 1, upper-right inset) shows that the full extent of the SETR and ETR is larger and longer (50–60 km long and 12–13 km wide) than the NWTR and SR (20–24 km long and 5–9 km wide). High-resolution bathymetry reveals that the shallow and intermediate parts of the SETR and ETR are characterized by gently sloping areas (<4°), that gradually deepen from the nearshore to the offshore without a clear gradient break (Fig. 1, see details in Quartau et al. 2014). Multibeam and side scan sonar surveys in the deeper parts of the SETR and ETR (Lourenço 2007; Miranda et al. 2012; Mitchell et al., Volcanism in the Azores: a marine geophysical perspective, unpublished) show smooth, terrace-like ridges mainly affected by tectonic features. In contrast, the SR and NWTR have a rugged surface, mostly formed by linear volcanic centers (Figs. 1 and 2; see section "Volcanic features"). A relatively wide flat area is also recognizable on the shallow and intermediate part of the NWTR, whereas a smaller flat area of erosive nature characterizes the summit of the SR (Figs. 1 and 2 and Quartau et al. 2014).

Between the four main ridges (i.e., in the inter-ridge areas), the shallow-water areas correspond to typical erosional insular shelves extending down to a sharp gradient break from −60 to −190 m (Fig. 1 and Quartau et al. 2014). Below the shelf edge, the submarine flanks are usually very steep (gradients up to 40°) and defined by an uneven morphology due to alternating sedimentary and volcanic features. A detailed description of the main volcanic, tectonic and mass-wasting features recognized on the Terceira offshore is presented in the following sections.

Volcanic features

A large number of volcanic features crop out offshore Terceira, covering about 30 % of the surveyed area and ac-counting for 480 km^2 (light-brown areas in Fig. 2). Besides lava flows on the insular shelf, commonly representing the progradation of subaerial lava flows into the sea (Quartau et al. 2014), and some other less common volcanic morphol-ogies present in deep-water, such as lava terraces in the lower flank of SR, the volcanic features can be divided into two main types: volcanic cones and linear eruptive centers (Figs. 2, 3, 4, 5, and 6).

Table 2 Spearman correlation matrix (half below the black cells) and p values (half above the black cells) for pointy cones, flat topped cones, and linear eruptive centers

Pointy cones	Summit depth (m)	Max. depth (m)	Height (m)	Max. diameter (m)	Min.diameter (m)	Area (m^2)	H/W ratio	Max./min. diameters	Average slope gradient (°)
Summit depth (m)		**0.000**	0.471	0.753	0.742	0.887	0.135	0.312	**0.047**
Max. depth (m)	0.921		0.010	0.026	0.113	0.054	0.046	0.327	0.015
Height (m)	0.070	0.248		**< 0.0001**	**< 0.0001**	**< 0.0001**	**< 0.0001**	0.090	**< 0.0001**
Max.diameter (m)	0.031	0.215	0.624		**< 0.0001**	**< 0.0001**	0.668	**0.002**	0.337
Min.diameter (m)	-0.032	0.154	0.704	0.750		**< 0.0001**	0.074	**0.001**	0.554
Area (m^2)	-0.014	0.187	0.722	0.923	0.897		0.314	0.885	0.454
H/W	0.146	0.193	0.717	0.042	0.173	0.098		**0.005**	**< 0.0001**
Max./min. diameters	0.098	0.096	-0.165	0.295	-0.330	0.014	-0.271		0.386
Average slope gradients (°)	0.192	0.236	0.402	0.094	0.058	0.073	0.506	0.085	

Flat-topped cones	Summit depth (m)	Max. depth (m)	Height (m)	Max.diameter (m)	Min.diameter (m)	Area (m^2)	H/W ratio	Max./min. diameters	Average slope gradient (°)	Top diameter (m)	Top/basal diameters
Summit depth (m)		0.151	0.171	0.752	0.977	0.703	0.069	0.428	0.462	0.267	0.132
Max. depth (m)	0.566		**< 0.0001**	0.096	0.069	**0.037**	**0.011**	0.171	0.083	0.752	0.151
Height (m)	0.539	0.994		0.096	0.069	**0.046**	**0.011**	0.171	0.069	0.840	0.171
Max.diameter (m)	0.133	0.639	0.635		**0.022**	**0.002**	0.536	0.619	0.267	0.703	0.267
Min.diameter (m)	0.012	0.683	0.690	0.8		**0.005**	0.536	0.665	0.428	0.840	0.360
Area (m^2)	0.156	0.755	0.738	0.922	0.905		0.462	1.000	0.243	0.582	0.428
H/W ratio	0.683	0.850	0.857	0.252	0.262	0.310		0.058	0.096	0.360	0.132
Max./min. diameters	-0.311	-0.527	-0.548	0.216	-0.190	0.000	-0.714		0.327	0.360	0.536
Average slope gradients (°)	0.313	0.669	0.695	0.452	0.335	0.479	0.635	-0.383		0.536	0.840
Top diameter (m)	-0.431	-0.120	-0.095	0.168	0.095	0.238	-0.381	0.381	0.252		**0.028**
top/basal diameters	0.599	0.563	0.548	0.443	0.381	0.333	0.595	-0.262	0.096	-0.786	

LEC	Summit depth (m)	Max. depth (m)	Height (m)	Max.diameter (m)	Min.diameter (m)	Area (m^2)	Average slope gradient (°)
Summit depth (m)		**0.000**	**0.020**	**0.001**	0.091	**0.002**	0.541
Max. depth (m)	0.936		**0.008**	**< 0.0001**	**0.007**	**< 0.0001**	0.553
Height (m)	0.306	0.349		**0.001**	**< 0.0001**	**< 0.0001**	**< 0.0001**
Max.diameter (m)	0.416	0.604	0.440		**< 0.0001**	**< 0.0001**	0.421
Min.diameter (m)	0.224	0.354	0.773	0.588		**< 0.0001**	**0.007**
Area (m^2)	0.392	0.586	0.618	0.926	0.8		0.116
Average slope gradients (°)	0.082	0.079	0.518	0.107	0.351	0.209	

The orange and green cells indicate correlation values≥0.5 and 0.8, respectively; yellow cells are used for negative correlation with values≤ 0.5. The lower *p* values are marked in bold, as they indicate a higher reliability for the statistical correlation

Volcanic cones

These are positive morphological features, with conical shapes. They are found in all the investigated submarine sec-tors, with the exception of the ETR (Fig. 2). The volcanic cones may be isolated, aligned along the main tectonic trend of the ridges, or occur in clusters (Figs. 2, 3, 4, 5, and 6). With a few exceptions, they lack a summit crater or collapse pit. Based on their morphology, volcanic cones can be divided into two main sub-types: pointy and flat-topped (Figs. 2, 3, 4, 5, 6).

Pointy cones A total of 108 pointy cones were recognized, with basal diameters ranging from 214 to 2,113 m, heights from 28 to 460 m, and planimetric areas from about 36×10^3 to $3{,}500 \times 10^3$ m^2 (Table 1). Their summit water depths vary between 17 and 2,400 m, even though most of them are at intermediate depths (median value of 522 m, Table 1). Pointy cones

commonly have smooth flanks, with gradients ranging between ~8° and 38° and aspect ratio (H/W) between 0.05 and 0.40, with a median value of 0.14. The base of the cones varies from circular to elliptical. The elliptical cones have their main axes trending N20°E–N157°E (median value N117°E) in the SR, and N124°E–N156°E (median value N133°E) in the NWTR (Fig. 7). A few elongated pointy cones are present at the western border of the SETR trending N140°E-N145°E (Figs. 2 and 3), whereas in inter-ridge areas more variable elongation trends are observed, ranging between N24°E and N180°E (median value N126°E, Fig. 7). The main morphometric parameters do not obviously vary systematically with water depth (Table 2, scatter plots a–e in Fig. 8). Correlations are observed between height and average basal diameter (Fig. 8f), and between maximum and minimum diameters (Fig. 8g), even if both distributions are scattered.

Flat topped cones A total of 10 flat-topped cones were rec-ognized on the SETR, NWTR and SR at depths between 12 and 215 m (Fig. 2, Table 1). Flat-topped cones are mostly circular and have average basal diameters of 647–2,355 m, heights of 15–210 m, and planimetric areas of about 329×10^3 to $4{,}350\times 10^3$ m^2 (Table 1). The ratio between basal and top diameters ranges between 1.2 and 4.7, while H/W ratio is 0.02–0.11. They commonly have smooth flanks, with gradi-ents ranging between 5° and 20°. Most of the flat-topped cones are characterized by irregular tops, with narrow, concentric ridges and furrows, and a small central mound is often present (Figs. 3 and 9a). Height, H/W ratio, and top/basal diameter vary somewhat with summit depth (Figs. 8a, 8e and Table 2). Some correlations are observed between the maximum depth (corresponding to the base of the cones) and most of the morphological parameters (Table 2), especially the height and H/W ratio. A correlation is also observed between average gradients and heights, whereas negative correlations are seen between the maximum/minimum diameter ratios against maximum depth, height, and H/W ratio (Table 2).

Linear eruptive centers (LEC)

These are positive volcanic structures, commonly elongated along the main orientation or tectonic trend of the large ridges (Figs. 2, 3, 4, and 5). LEC are found between −200 and −2, 400 m, although they commonly occur in intermediate-deep water (median value of −648 m, Table 1). They are 116–926 m wide, 477–6,315 m long, 13–225 m high, and cover planimet-ric areas of about 60×10^6 to 3600×10^6 m^2. In particular, the average length of the LECs (around 1.5 km, Table 1) is in the range of values measured for hummocky ridges of MAR (1–2.5 km), whereas longer features (up to 6 km, Table 1) are comparable with hummocky ridges observed in Galapagos (e.g., Colman et al. 2012).

Their flanks show both smooth and uneven morphology, with gradients of 15°–42° (median value of 25°). In detail,

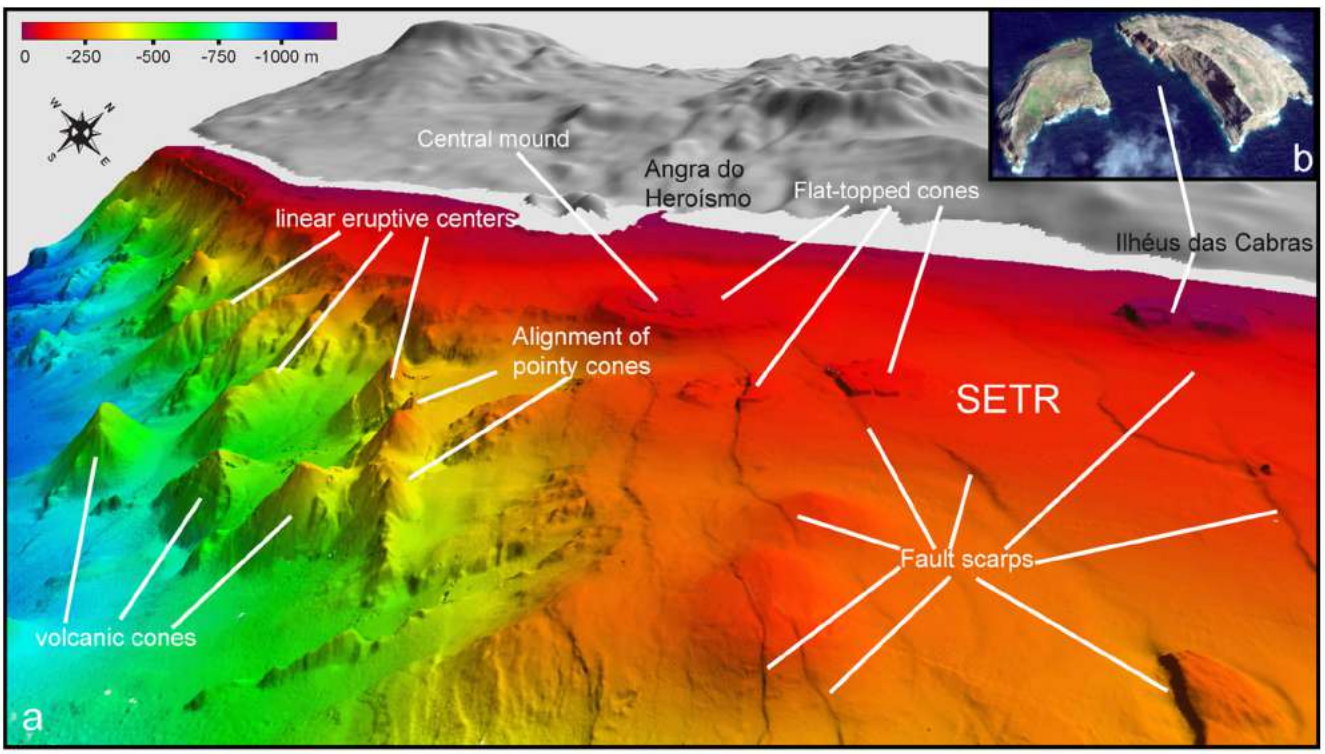

Fig. 3 3 D view of the South East Terceira Ridge (**a**) showing several volcanic and tectonic features (see text for details); vertical exaggeration ×1.5. Oblique photos of tuff cones of Ilhéus das Cabras (**b**), bisected by faults

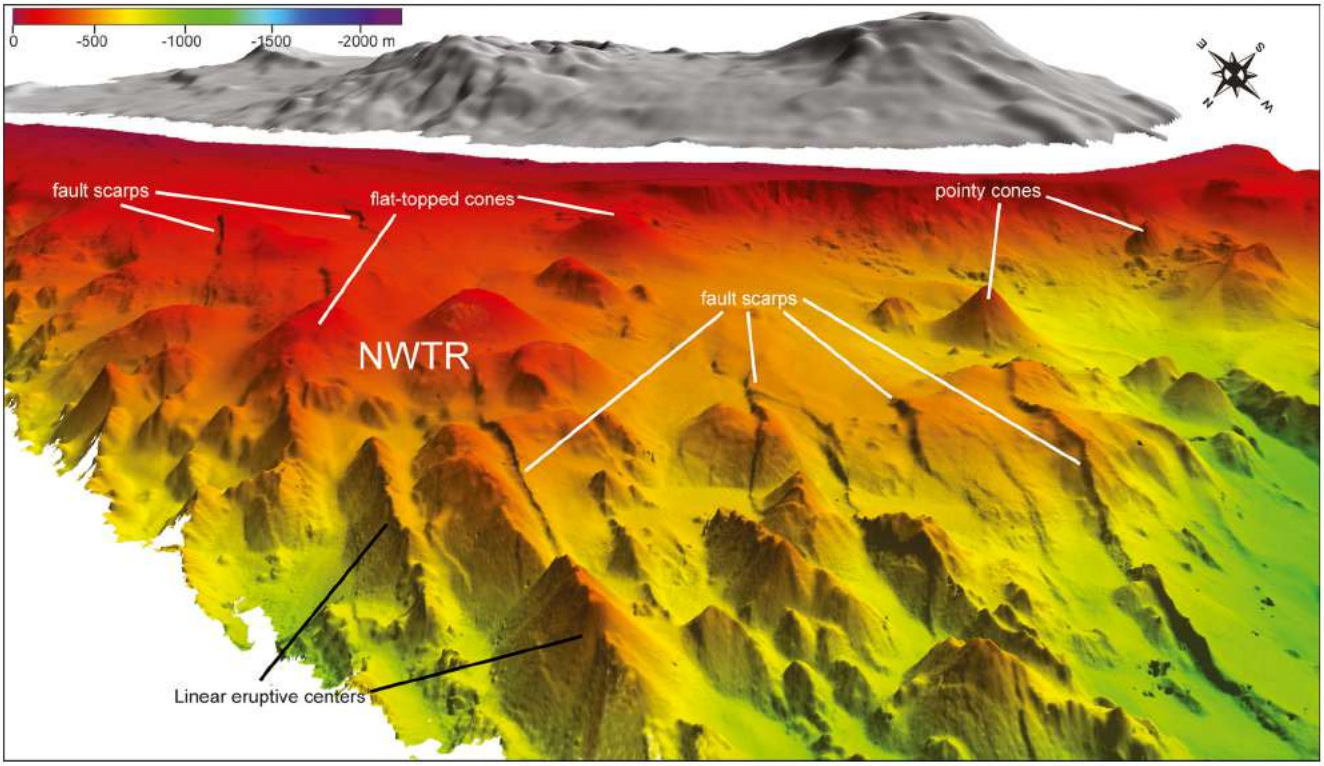

Fig. 4 3 D view of the North West Terceira Ridge, where fault scarps affect flat topped cones, and linear eruptive centers are present downslope (see text for details); vertical exaggeration ×1.5

10 LECs were identified in the NWTR, trending N133°E–N159°E (median value, N141°E; Fig. 7), whereas 38 features trending N90°E–N179°E (median value, N133°E) are present in the SR. A larger variability in strike is observed for the 11 LEC formed in the inter-ridge areas (Fig. 7), similar to the reported for the volcanic cones. The main morphometric parameters have no clear relationship with the summit and maximum depths (scatter plots a–e in Fig. 8, Table 2), with the exception of a slight correlation of the maximum depth with the area and maximum

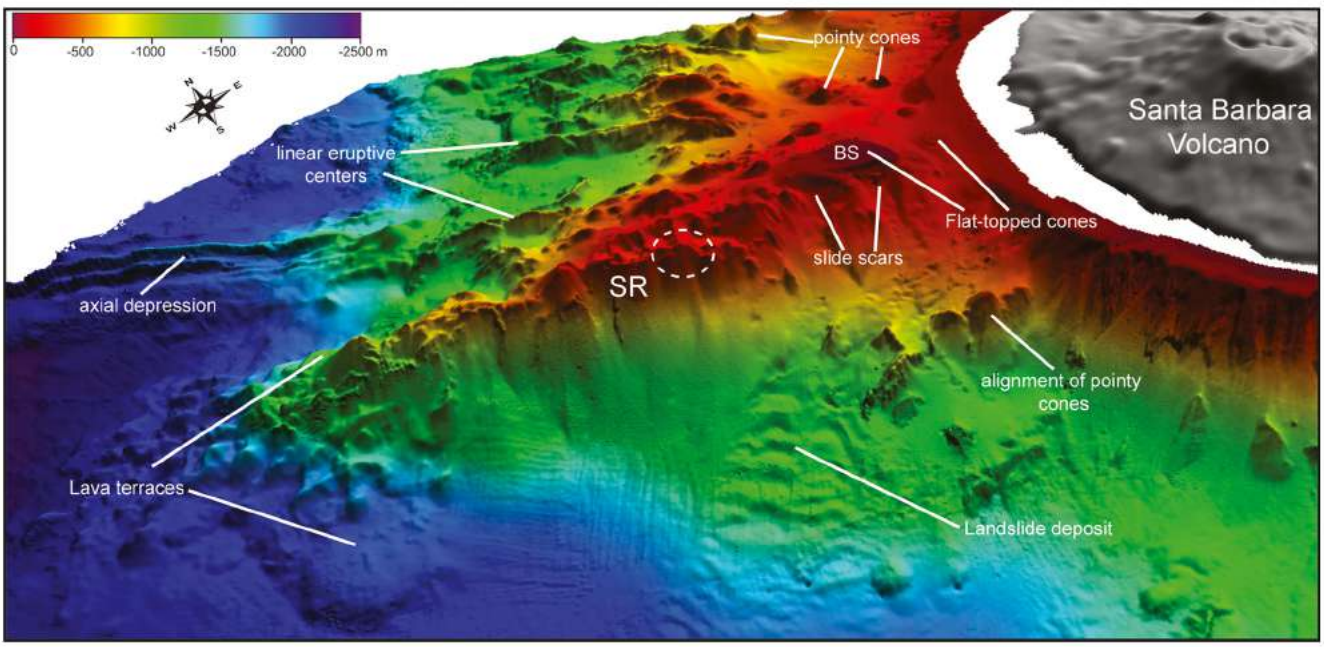

Fig. 5 3 D view of the Serreta Ridge (*SR*), where several volcanic features and two around 1 km wide landslide scars are present (see text for details); vertical exaggeration ×1.5. *BS*: Baixa de Serreta. The *white dashed ellipse* roughly indicates the area of the 1998 2001 submarine 'lava balloon' eruption

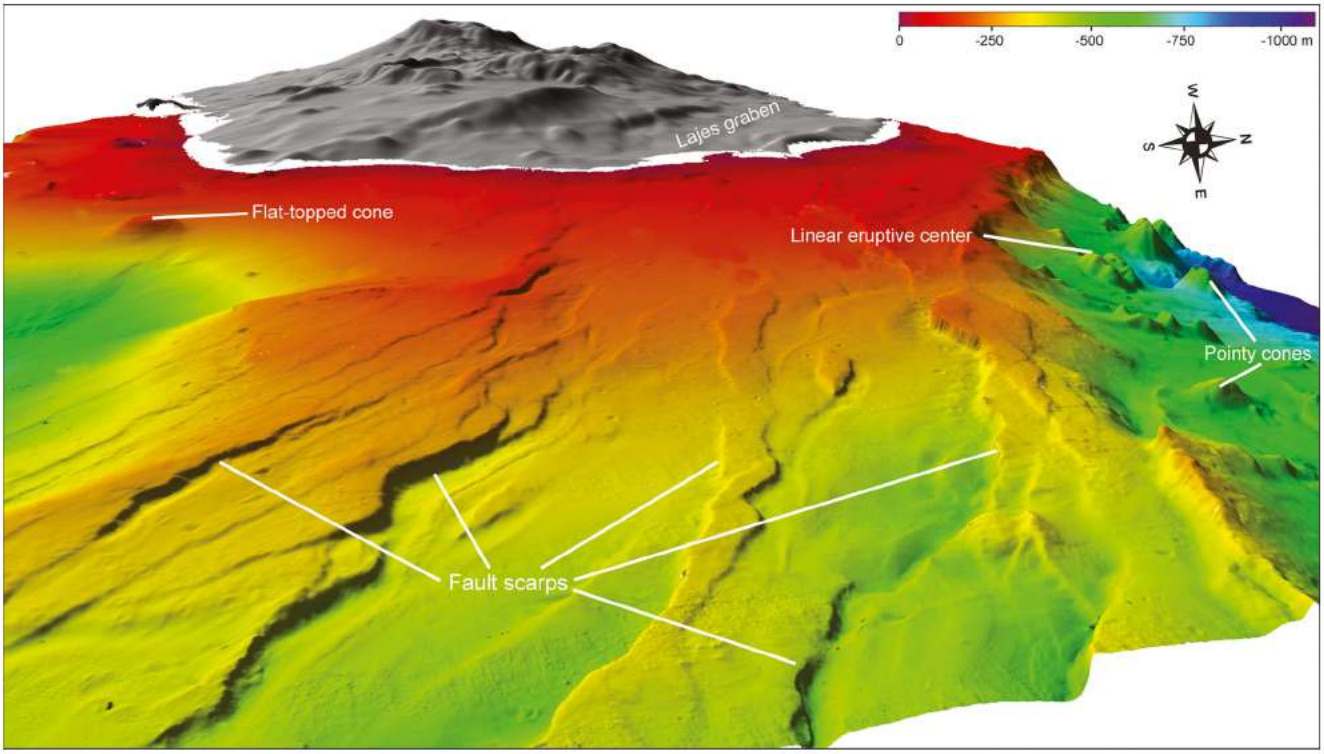

Fig. 6 3 D view of the East Terceira Ridge, where fault scarps off the Lajes Graben are evident (see text for details); vertical exaggeration ×1.5

diameter. Correlations are seen for height against average gradients and area (Table 2).

Elongated and uneven LEC were observed in the intermediate/deep-water sector between the SR and the NWTR (Figs. 2 and 5). The summit of these features is commonly characterized by a positive rise or, alternatively, by a slightly depressed area. The largest structure is located north of the SR between −1,800 and −2,400 m and characterized by a rifted summit, i.e., an axial depression. This depression is 200–300 m wide, 7 km long, and up to 100 m deep, delimited by two steep, linear scarps (axial depression in Fig. 5), some-how similar to volcanic edifices at the MAR with grabens on the summits.

Tectonic features

A large number of fault scarps displacing the seafloor were observed on the SETR and ETR (Figs. 3 and 6, respectively), and less frequently in the NWTR (Fig. 4). Most faults are normal, even if some in the Lajes Graben show morphologies with bends suggesting dextral strike slip (Fig. 2), in agreement with neotectonic studies of onshore Lajes Fault, where slickensides indicated both normal and oblique (with dextral component) displacement (Madeira et al., unpublished).

In detail, a set of 56 fault scarps trending between N96°E and N144°E was recognized on the ETR off the Lajes Graben (LG; Figs. 2, 6, 9c, d and 10). These faults, dipping in opposite

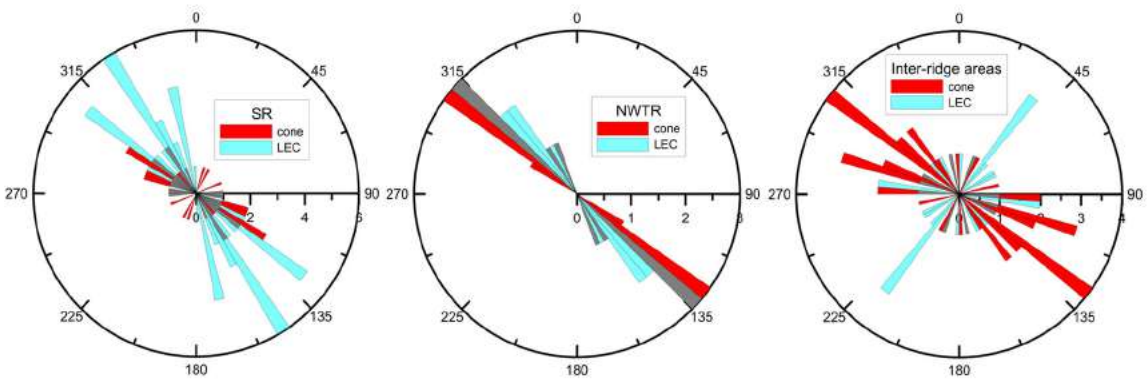

Fig. 7 Rose diagrams summarizing the strikes of elongation for pointy cones (*red*) and linear eruptive centers (LEC, *light blue*) for the Serreta Ridge (*SR*), North West Terceira Ridge (*NWTR*) and inter ridge areas. The *gray areas* indicate the overlapping sectors of cones and LEC

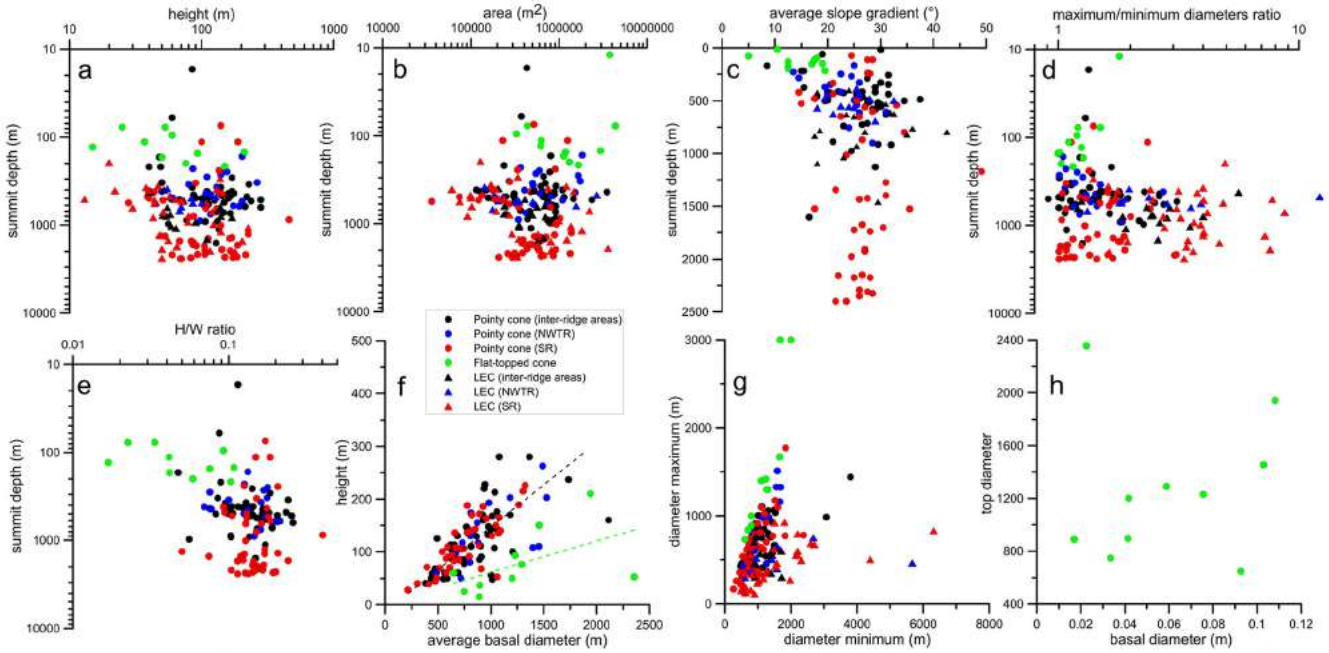

Fig. 8 Scatter plots of the main morphometric parameters measured for volcanic cones and linear eruptive centers (*LEC*). Note that height, area, average slope gradient, maximum/minimum diameters ratio vary non systematically with summit depth, whereas a weak correlation is present between aspect ratio and summit depth. Correlations are present between height and average basal diameter of cones as well as between minimum and maximum diameter, even though distributions are quite scattered. In scatter plot **f**, note the difference in height/average basal diameter ratios between pointy and flat topped cones evidenced by fitting the least squares lines (*black* and *green dashed lines*, respectively)

senses (roughly SW and NE), are 450–9,350 m long and have a relief at the surface of between 2 and 87 m (Fig. 10); the superficial offset increases seaward (Fig. 6).

A set of 38 fault scarps trending between N121°E and N171°E and mainly dipping towards NE was recognized on the SETR (Figs. 2, 3, 9a, b and 10). Most scarps affect the submarine flat-topped cones, sometimes bisecting these features as observed in Fig. 3a or even more spectacularly in the subaerial tuff cone of Ilhéu das Cabras in Fig. 3b. In some cases, the faults apparently affect the sedimentary cover, as observed in Fig. 9b. These faults scarps are 660–5,000 m long, and have a relief at the surface of between 1 and 54 m (Fig. 10).

A set of 20 fault scarps trending between N112°E and N163°E are present on the NWTR (Figs. 2, 4, and 9e). Two sets of normal faults, dipping in opposite senses, were identified: NE-dipping faults are prevalent, whereas SW-dipping faults are markedly subordinate (Fig. 10). The fault scarps are 328–4,717 m long and have a relief at the surface between 2 and 50 m (Fig. 10). In shallow-water, some fault scarps cut volcanic cones, whereas downslope they cross along fresh-looking, elongated volcanic features (Fig. 4).

Mass-wasting features

The most common instability features found in the Terceira offshore are few hundred-meters wide superficial landslide scars affecting the edge of the insular shelf in the inter-ridge areas (Fig. 2 and Quartau et al 2014). These scars commonly represent the headwalls of channels developing downslope; sometimes the channel floor is characterized by a train of downslope asymmetric crescent-shaped bedforms, with wave-lengths of tens or few hundreds of meters, wave heights of a few meters and lateral extents of hundreds of meters (Chiocci et al. 2013).

Large-scale summit or flank collapses have not been identified in the multibeam bathymetry, with the exception of two landslide scars, 1–2 km wide, imaged on the upper part of the southern slope of SR between −100 and −600 m (Figs. 2 and 5). Downslope of the headwall scars, the landslide deposits cover an area of about 30 km^2 and are superficially characterized by an uneven morphology, defined by concave and convex down-slope asymmetric waveforms, with wavelengths of 500–800 m and wave heights of 20–50 m (Fig. 5).

Discussion

Distribution of volcanic features and tectonic control

The distribution and shape of the different volcanic and volcano-tectonic features recognized offshore Terceira provides valuable insights into the interaction between magmatism and tectonics in the formation of the volcanic ridges. This, in turn, may be related to the orientations and magnitudes of regional lithospheric stresses and basement

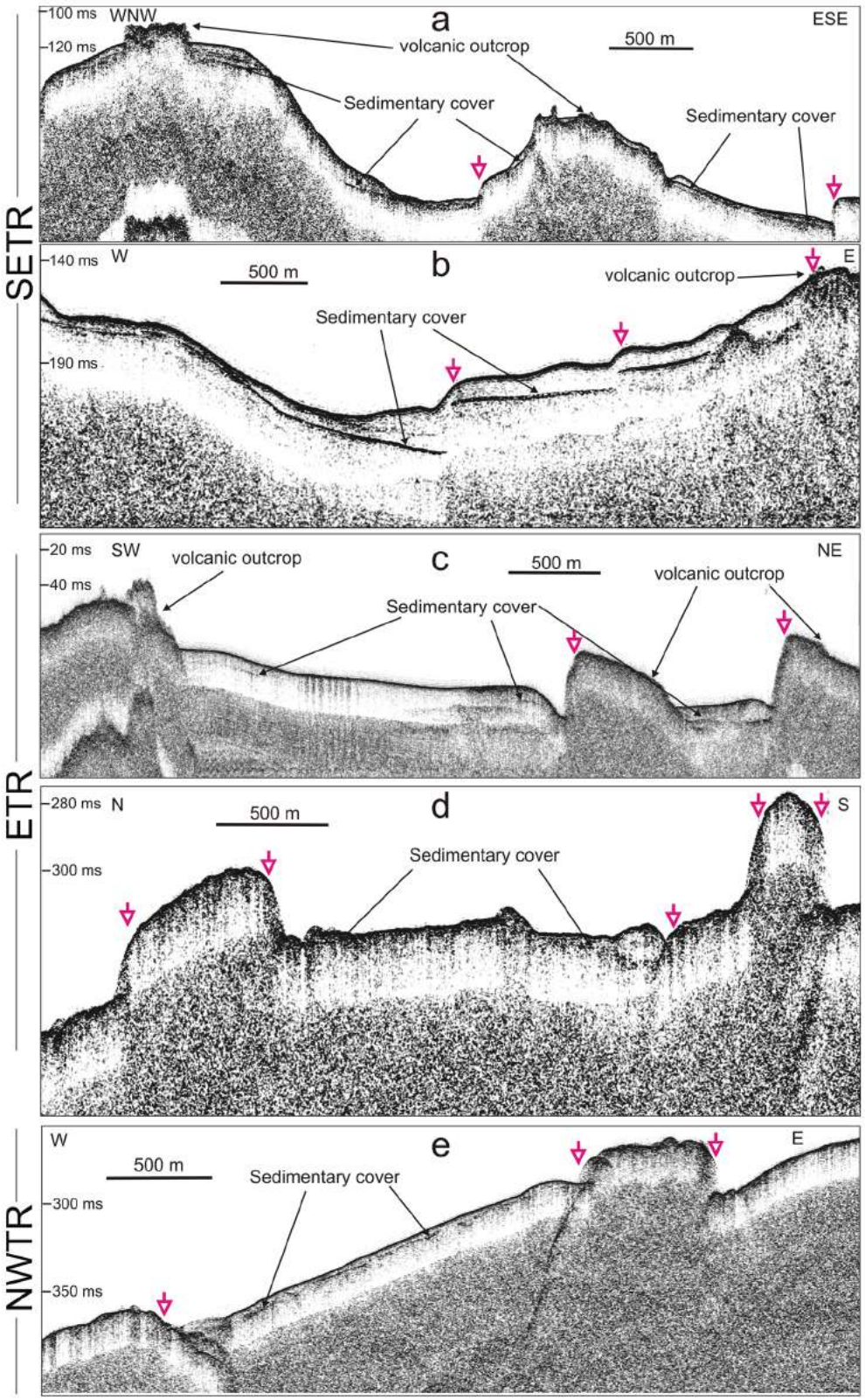

Fig. 9 CHIRP profiles across the main volcanic and tectonic features observed offshore Terceira (location in Fig. 1). The *magenta arrows* indicate fault scarps. On CHIRP profiles, the base of the recognizable sedimentary cover is indicated by *black arrows*, varying between some meters (profiles **a**, **c**, **d** and **e**) up to 15 m (profile **b**)

structures. The elongated morphology of most volcanic fea-tures offshore Terceira is a common characteristic seen in linear volcanic ridges elsewhere (e.g., Höskuldsson et al. 2007; Searle et al. 2010). These are formed by systems of volcanic and tectonic fissures (Gudmundsson 1986), which provide a preferential pathway for the ascent of magmas

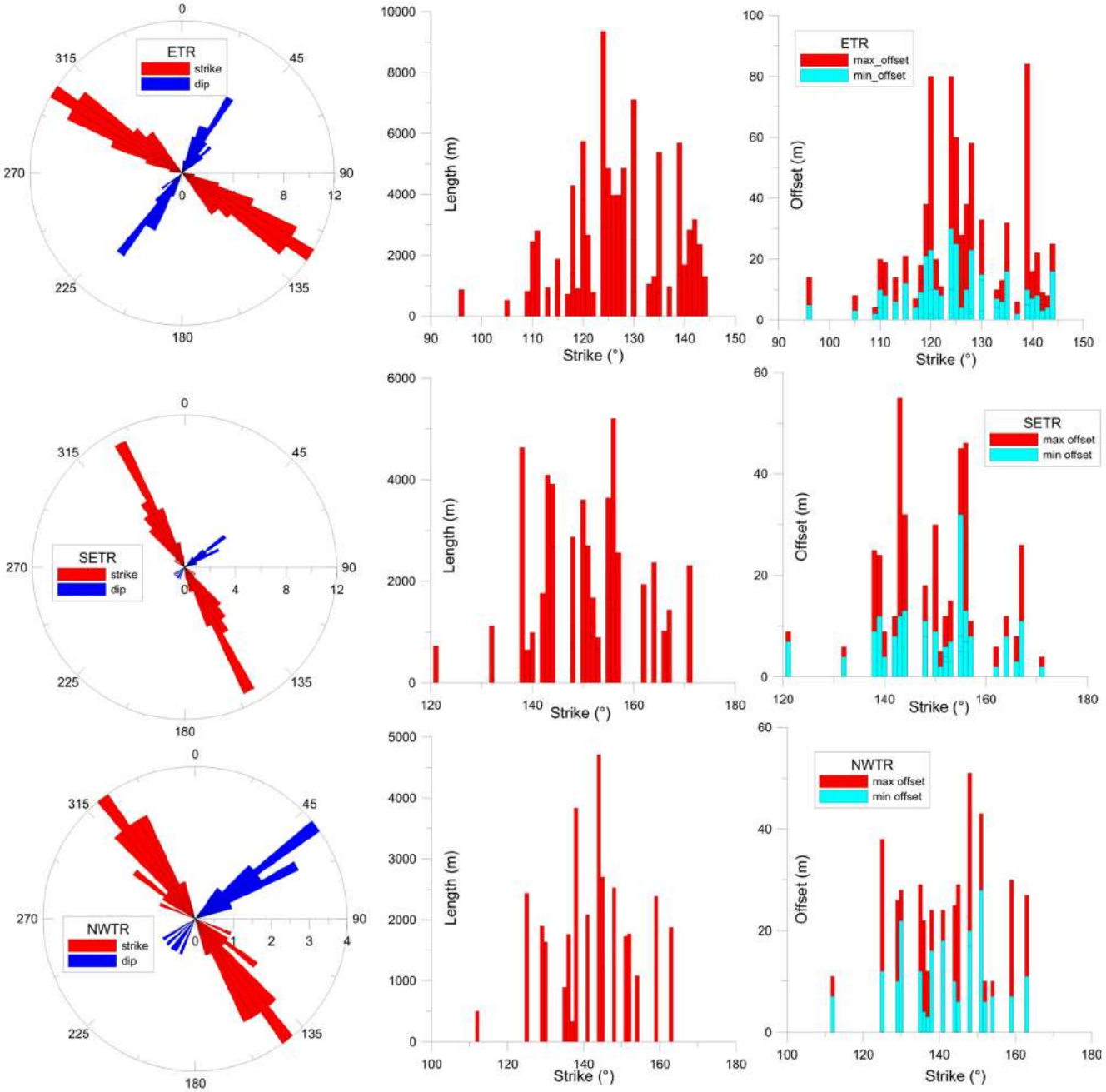

Fig. 10 On the left, the rose diagrams show the strike and dip direction of tectonic features (56 fault scarps for ETR, 38 for SETR and 20 for NWTR); on the right, histograms show the length, maximum and minimum offset of the fault scarps with respect to their strike

through the crust (e.g., Tempera et al. 2013; Zanon and Pimentel 2015). The elongated morphology of the volcanic features can occur either by eruptions along linear vents, as seen for instance in subaerial fissure swarms in Iceland and Azores (e.g., Gudmundsson 1986; Smith and Cann 1993; Walker 1999), or by the overlapping of linear chains of pointy cones, or even as central volcanism focused on a single frac-ture (Briais et al. 2000; Smith and Cann 1993). Similarly, the alignment of pointy cones along preferential trends (Figs. 2, 3, 4, and 5) is a strong evidence of the regional tectonic control exerted on magma emplacement. In such cases, the formation of lineaments of isolated cones may be due to the rapid cooling of an eruptive fissure, favoring the progressive blocking of magma ascent through a dyke, leading to the centralization of eruptive vents (Head et al. 1996). A swift transition from line- to point-source eruptions was observed during subaerial basaltic fissure eruptions in Iceland (e.g., Andrew and Gudmundsson 2007) and Hawai'I (e.g., Lockwood et al. 1987). It is also worth noting that these small-scale elongated volcanic features are parallel to the large ridges and to many of the normal faults affecting the seafloor. Because a fluid-filled crack cannot sustain shear stresses, the

orientations of dykes should reflect the orientations of the principal stress axes. Therefore, the common orientation of these features would suggest that tectonic stresses were perpendicular to the large ridges at the times of eruption.

Most of the volcanic features occur off the north-western sector of Terceira (area between SR and NWTR, Fig. 2), mainly trending N120°E to N150°E, which is consistent with the strike of the main regional tectonic structures observed at the TR and more generally in the Azores Plateau (e.g., Lourenço et al. 1998; Miranda et al. 1998). Nevertheless, alignments of cones along different directions from the main regional trends were also observed, such as in the inter-ridge areas (northern and southern sectors of Terceira). Here, volcanic features occur radially to the flank of the main subaerial volcanic edifices, suggesting that they may result from local magmatic stress due to emplacement of the edifice and reflect the interactions between regional and local magmatic stresses (e.g., Bacon et al. 1980; Tibaldi and Lagmay 2006).

Very few lava terraces were observed offshore Terceira Island (in the lower flanks of SR, Fig. 5), similarly to that reported for Pico Ridge and Condor Seamount (Stretch et al. 2006; Tempera et al. 2013, respectively). In contrast, lava terraces and flat-topped seamounts are more common in other volcanic ridges, such as Reykjanes Ridge, Puna Ridge and Hawaiian Archipelago, (Parson et al. 1993; Smith and Cann 1999; Clague et al. 2000). In Galapagos, the formation of these features characterized by small height/diameter ratios has been associated to high effusive rates associated to areas with high magma supply (McClinton et al. 2013). In Azores, the paucity of these features has been tentatively interpreted as the result of a lower volatile content in the Azorean magma, hindering long-lived eruption (Stretch et al. 2006). Typical basaltic eruptions in Azores do not exceed 0.1 km^3 dens rock equivalent (DRE) (e.g., Self 1976, Booth et al. 1978). Zanon and Pimentel (2015) showed that magmas are stored at depth in small, isolated batches at fissure zones.

Relationship between morphology of volcanic features and water depth

An overall progressive change with decreasing water depths is observed offshore Terceira from large and complex volcanic features in deep-water, sometimes with an axial depression at the summit to LEC, pointy cones and flat-topped tuff cones (Figs. 1 and 2). This may be interpreted as a result of the interaction between different hydrostatic pressures and crustal thickness (Fig. 11), similar to the suggestion for Condor Seamount by Tempera et al. (2013). A higher hydrostatic pressure reduces gas exsolution from magma favoring effusive eruptions (e.g., Fisher 1984); a thinner homogeneous crust allows intruding dykes to reach the seafloor more easily, without major obstacles, directly feeding fissure eruptions. Together, these factors may lead to the preferential formation of large elongated ridges and LEC in deep-water sectors (Fig. 11). Colman et al. (2012) and Mcclinton et al. (2013) found that fissure eruptions in Galapagos were longer when effusion rates were higher. In contrast, the progressive increase in crustal thickness and rheological complexity should have strong effects on the magmatic plumbing system (Lourenço 2007) encouraging the establishment of more centralized eruptive systems, preferentially forming isolated or aligned volcanic cones (Fig. 11). Pointy cones are found in all water depths shallower than about 2, 500 m (Table 1) and their morphometric parameters (Fig 8 and Table 2) do not show any relationship with summit depth, suggesting that a common eruption mechanism may be respon-sible, similar to that proposed for the submarine cones at Pico Ridge (Stretch et al. 2006). However, we are aware of the strong limitations of inferring eruptive styles based only on the analy-sis of bathymetric data.

Recent marine studies at the Galapagos (e.g., Colman et al. 2012; McClinton et al. 2013) have shown that the style of eruptions and the mode of lava emplacement are mostly controlled by the rate of supply of magma to a volcanic ridge. Moreover, other factors may locally control individual eruptions, as suggested by the large spectrum of eruption styles occurring within ridge segments characterized by similar magma supply (McClinton et al. 2013). The eruptive styles can be governed by the interplay of conditions as viscosity of the melt, its composition and temperature (e.g., Bonatti and Harrison 1988). In addition, the rapidity of volcanic ascent and eruption leads to a number of consequences for the flow of magma, as well as the content and exsolution of volatiles in relation to the confining pressure of the water column.

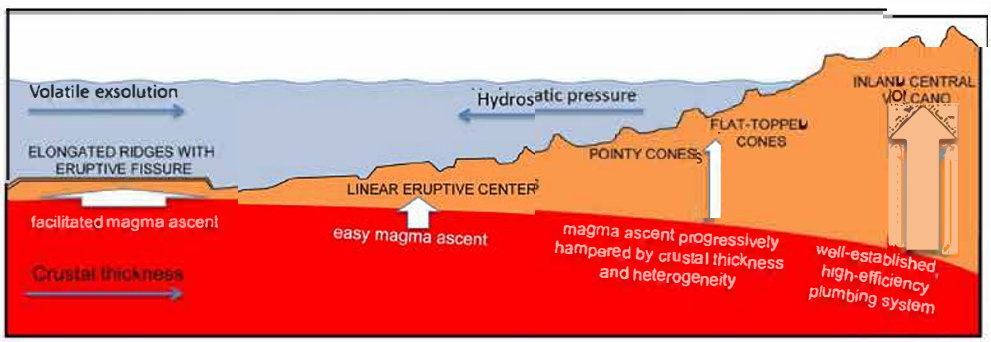

Fig. 11 Conceptual sketch summarizing the progressive change in dominant volcanic features offshore Terceira with water depth (see text for details)

In contrast, flat-topped cones are mainly limited to shallow depths (shallower than 220 m, Table 1) and their morphometric parameters (height, H/W ratio, and top/basal diameter ratio) show correlations with summit depth (Figs. 8a, e and Table 2), suggesting that this may play an important role in their formation. Most of the flat-topped cones recognized (especially on the SETR, Fig. 3) can be interpreted as tuff cones formed during surtseyan eruptions. Their flat summits are characterized by sub-concentric furrows and ridges, and other small circular features, that likely arose from episodic eruptions into shallow water and subsequent wave erosion, as observed at Surtla, Iceland (Kokelaar and Durant 1983), or at Ferdinandea (Coltelli et al. 2012). Erosion of individual pyroclastic layers with varying resistance on their summit may leave the concentric furrows and ridges (e.g., Mitchell et al., unpublished). Similarly, the small-scale relief commonly found on the shallowest parts of the cone summits may be interpreted as remnants of the central vent left by differential erosion (e.g., Mitchell et al. 2012a). The large amount of pyroclasts forming these submarine flat-topped cones could have been easily eroded by wave action during Late-Quaternary sea level fluctuations, leading to the formation of summit planar surfaces (Fig. 9a). A recent example of a similar process probably occurred at the Baixa da Serreta bank (BS in Fig. 5) on the SR, the probable site of the 1867 submarine eruption (Weston 1964). Here, the planar surface iden-tified at −30/−40 m can be considered to be result of wave erosion of scarcely cohesive volcanic products (Quartau et al. 2014), similarly to what was observed at Dom João de Castro bank in 1720 (Weston 1964; Pascoal et al. 2006) or, more recently, at Surtla and other satellite vents of Surtsey volcano in 1963–1966 (Kokelaar and Durant 1983). Even if erosion is predominantly responsible for the modeling of flat-topped cones, other factors such as the forced spreading of eruptive columns on reaching the water–air density barrier may be considered (Cashman and Fiske 1991; Tables 1 and 2). This mechanism implies a wider dispersion of particles away from the vent in shallow-water, as recently proposed for the forma-tion of similar flat-topped cones at the Pico Ridge shallower than −300 m (Mitchell et al. 2012a). The combined effect of wave erosion and forced spreading of eruptive columns would favor the preferential deposition of pyroclastic material on the flanks of these cones (Fig. 8c and Table 1).

One of the main parameters used for the morphometric characterization of volcanic cones is the ratio between cone height and average basal diameter (e.g., the aspect ratio H/W, see Favalli et al. 2009). In offshore Terceira, a slight positive correlation between these two parameters is seen (Fig. 8f), even if their distribution is quite scattered, with H/W values ranging between 0.01 and 0.4 (Fig. 8e). The median value of 0.14 for the H/W ratio is low with respect to the classic value of 0.18 reported for subaerial volcanic cones (e.g., Porter 1972; Settle 1979), but it is within the range (0.1–0.3) reported for submarine cones in the Azores (Stretch et al. 2006; Tempera et al. 2013) and other submarine volcanic settings (e.g., Kelly et al. 2014). Moreover, the lack of a constant relationship between these parameters (Fig. 8f) suggests that the cones do not develop in a simple self-similar way, as previously reported for the volcanic cones on Pico Ridge (Stretch et al. 2006).

The apparent absence of summit craters or collapse pits on both conical and linear edifices could indicate the lack of drain back of magma into the magma chamber and/or an overall low explosivity. This latter could be due to the confining pressure associated with the water depth, but could also reflect the predominantly alkaline composition of the magmas (basaltic *sensu latu*). This is supported by geochemical analyses of samples recovered inland (e.g., Beier et al. 2008; Zanon and Pimentel 2015) and during the 1998–2001 submarine eruptive crisis (e.g., Kueppers et al. 2012; Zanon and Pimentel 2015), as well as from similar submarine cones at Pico Ridge and Condor Seamount (Stretch et al. 2006; Tempera et al. 2013). However, these morphological features may have been masked by successive volcanic or erosive-depositional processes, or might not be recognizable in deep-water due to the decrease of multibeam resolution with depth. The past occurrence of highly explosive eruptions at Terceira Island is supported by the presence of several caldera-complexes and widespread outcropping of tephra and ignimbrite deposits (Self 1976; Gertisser et al. 2010).

Tectonic features and morpho-structural differences between the ridges

Two main sets of normal faults, trending WNW–ESE and NNW–SSE, were recognized offshore Terceira (Figs. 2 and 10), consistent with the elongation direction of the previously described volcanic features (section Distribution of volcanic features and tectonic control), and more generally with the regional fault systems identified in the Azores Plateau (e.g., Lourenço et al. 1998). Within the same ridge only one fault system is present and is roughly aligned with each ridge overall direction. The WNW–ESE set dominates the ETR and the SR and the NNW–SSE set dominates the SETR and the NWTR (Figs. 1 and 2). Nonetheless, both structural trends were recognized onshore Terceira Island (Madeira 2005; Madeira et al., unpublished) that lies at the intersection of the four ridges (Fig. 1). The volcano-tectonic setting of the island is yet more complicated, as witnessed by the co-existence of previous regional trends of N–S and NE–SW volcano-tectonic structures (Madeira et al., unpublished), and the overall E–W shape of the island, resulting from the overlapping of the four central volcanoes (see section Geological setting). The Faial Island also has multiple structural trends, lying at the intersection of the main regional trend WNW–ESE with the minor NNE–SSW trend, and

where other directions related to local magmatic stresses are present (Trippanera et al. 2014).

In near-shore areas, faults are mostly hidden by the sedi-mentary cover and recent volcanic deposits, whereas their morphological expression is more remarkable in offshore gently sloping areas, with less sedimentary cover (Figs. 2, 3, 4, and 6). Their lengths (328–9,350 m) and superficial offsets measured from bathymetry (1–84 m) are in the same range of the Holocene normal faults at the rift zone of Iceland (e.g., Gudmundsson 2000). Moreover, even if the distribution is quite scattered, we note a good correlation between the two parameters (Fig. 12), similarly to that observed for normal faults in Iceland (Gudmundsson 2000 and 2005; Gudmundsson et al. 2013). The length–displacement ratios of the faults observed in the Terceira offshore range between 24 and 800 m, being larger than the values found in literature (10^1–10^2 m, Clark and Cox 1996; Schlische et al. 1996; Gudmundsson et al. 2013). These high values can be ex-plained by transtensive regime of Azores boundary resulting in lower displacements relatively to length of the faults be-cause deformation is also accommodated through horizontal displacement (strike-slip). However, it is important to consider that most of the offsets are measured from bathymetry, so implying that these ratios might be biased towards higher values, especially for faults in near-shore areas where sedi-mentary cover is thicker.

On the ETR, we observed the longest faults forming a series of horst and graben structures, related to the onshore Lajes Graben (Figs. 2 and 6). This onshore structure is part of a larger graben system recognizable in the surrounding sub-marine areas (Fig. 2 and Quartau et al.

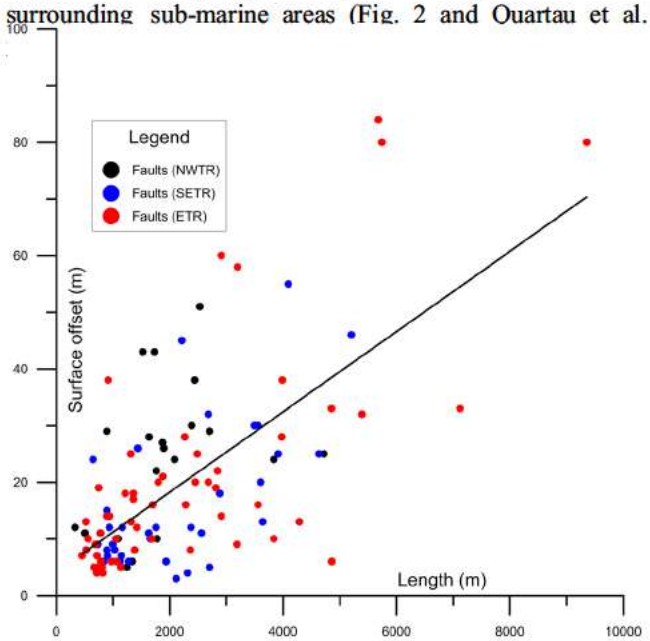

Fig. 12 Scatter plot of length versus surface offset (assumed as a minimum value for total displacement) for fault scarps at Terceira offshore. Acronyms as in the previous figures

is widely disrupted by faults, as witnessed by the high-resolution bathymetry (Figs. 2 and 3) and the deep-tow side scan sonar survey (Lourenço 2007; Mitchell et al., unpub-lished). In contrast, in the NWTR, superficial faults are visible but less common and in the SR they are not recognizable at all, whereas volcanic structures related to fault-controlled fissure eruptions are dominant.

These marked volcano-tectonic and structural differences between the four ridges support the hypothesis that they might have developed independently, possibly each representing a successive stage of ridge evolution. This staged development is similar to that proposed to explain the origin of crossing structures observed on axial volcanic ridges of the MAR by Parson et al. (1993). The broader SETR and ETR, character-ized in their upper and median parts by a significant sedimen-tary cover, with scarce superficial volcanic features and wide-ly affected by faulting, are probably in a mature stage of de-velopment. The narrower NWTR, characterized by faulting, sedimentary cover down to −300/−400 m and fresh-looking volcanic features at greater depth, can be considered in an intermediate stage of evolution. Finally, the scarcity of super-ficial tectonic features, together with the rugged morphology of the SR, suggests that it is still in a relatively early stage of its evolution. The SR could represent the western extension of the recent BFS, as witnessed by the widespread, fresh-looking volcanic features (Figs. 2 and 5, section Distribution of volcanic features and tectonic control) and the occurrence of the most recent submarine eruptions (1867 and 1998–2001) in the SR (e.g., Weston 1964; Kueppers et al. 2012).

In agreement with the proposed model, the SR and the NWTR ridges show high-amplitude magnetic anomalies (Fig. VI.1 in Lourenço 2007) and well-defined volcanic cones and LEC, suggesting their recent activity. The SETR also shows strong positive anomalies, but fewer volcanic cones and is eroded and offset by faults. The ETR has almost no volcanic cones and has subdued positive to negative magnetic anomalies, with the exception of the nearshore part that has clear positive anomalies, related to the extension of recent subaerial lava flows into the sea. Therefore, we envisage that the ETR may primarily correspond to the Matuyama magnetic epoch (>0.78 Ma), being the oldest ridge; the SETR was al-ready formed during the Brunhes magnetic period (<0.78 Ma) but is now probably inactive, whereas the SR and NWTR ridges have started forming very recently and are still active. Strong negative anomalies between the SR and NWTR are incompatible with this interpretation (Fig. VI.1 in Lourenço 2007), although fresh volcanic morphologies are observed here. However, recent extensional processes acting in the Azorean segment of the EU-NU plate boundary may have split magnetization polarity pattern of the EU plate as the triple junction jumped northwards, from the East Azores Fracture Zone (Fig. 1) to its current position (Luís and Miranda 2008). Therefore, one can argue that in areas of recent rifting, the

interpretation of anomalies of the rifted basement can conceal the signal of recent and still incipient volcanic activity.

Mass-wasting processes

The lack of large-scale instability features around the Terceira submarine flanks differs from what is commonly reported for other volcanic islands, whose flanks are often dominated by large-scale sector collapse scars and related debris avalanche and flow deposits (Moore et al. 1994; Masson et al. 2002; Oehler et al. 2008; Romagnoli et al. 2009a and 2009b; Montanaro and Beget 2011). The lack of large-scale instability processes is probably related to the low height and relatively gentle slope of the central volcanic edifices, as supported by recent studies on the susceptibility of mid-ocean ridge volca-nic islands and seamounts to large-scale landsliding (Mitchell 2003). In addition, the very recent volcanism reported in al-most all the islands may contribute to obliterate these evidence (Mitchell et al. 2012b). The only case where such process has been recently identified is the steep-sided Pico Island (e.g., Hildenbrand et al. 2012; Mitchell et al. 2012b; Costa et al. 2014). Only a few 1-kilometer wide scars have been identified on the steep southern flank of the SR (Fig. 5). Here, the stepped morphology observed within the landslide deposits can be interpreted as the result of a slumping analogous to that observed along the steep submarine flanks of volcanic edifices in the South Sandwich arc (Leat et al. 2010) and Aeolian islands (Casalbore et al. 2014a). Minor instability processes were identified at the edge of the insular shelf surrounding Terceira Island, similar to those reported for other active vol-canic islands (Casalbore et al. 2011, 2014b; Quartau et al. 2010, 2012, 2014; Romagnoli et al. 2013). This is probably because these areas commonly have steep gradients and non-cohesive sediments near the shelf edge. Triggering mechanisms may include eruptive or seismic shacking as well as cyclic load-ing due to storm-waves. Some of these mass-wasting events are likely very recent, as witnessed by the presence of downslope asymmetric waveforms similar in size and morphology to cyclic steps observed in active canyon heads at continental margins (Paull et al. 2010; Casalbore et al. 2014c) and volcanic settings (Babonneau et al. 2013; Casalbore et al. 2014d; Romagnoli et al. 2012), considered to be indicators of recent sedimentary flows.

Conclusions

Morphologic information from high-resolution bathymetric data offshore Terceira has enabled us to reconstruct the main volcanic and tectonic processes characterizing the four sub-marine volcanic ridges, as well as their interaction with the island. The strike of linear volcanic centers and fault scarps was used as a tectonic marker for the stress field, revealing two main systems trending WNW–ESE and NNW–SSE, con-sistent with the regional tectonic structures affecting the Azores Plateau and related to a diffuse dextral transtensional zone (e.g., Lourenço et al. 1998). Only in the inter-ridge areas was there a larger dispersion of strike, possibly indicating the interaction between regional and local stresses due to the em-placement of the onshore central volcanoes.

The submarine ridges show marked differences in their size and shape, as well as in the distribution of volcano-tectonic features, probably reflecting different stages of formation. The suspected younger ridge (i.e., the SR) shows a strongly elon-gate shape and is punctuated by fresh-looking volcanic fea-tures, whereas evidence of tectonic and sedimentary features is scarce or confined to shallow-water areas. The intermediate-age ridge (i.e., the NWTR) is wider and characterized by an upper part with significant sedimentary cover, whereas fresh-looking LEC and tectonic features are present at greater depths. Mature ridges (i.e., the SETR and ETR) are signifi-cantly larger and have a smooth, flatter, terraced morphology. They are characterized by large gently sloping areas, with the sedimentary cover affected by pervasive fault scarps, and sub-ordinate volcanic features (mostly tuff cones, partly obliterat-ed by wave erosion).

At a finer scale, a progressive change is observed from large and complex, elongate ridges to LEC, pointy and flat-topped cones towards the coast (Fig. 11). The type of volcanic features offshore seems to be mainly controlled by the inter-action between different factors, particularly crustal thickness and hydrostatic pressure. At greater depths, the thinner crust should favor the propagation of dykes directly to the seafloor, whereas the increase in crustal thickness towards the island should constrain dyke intrusion into a few persisting path-ways, thus leading to more-centralized eruptions. The hy-drostatic pressure predominantly affects the exsolution of volatiles from the magma, favoring the formation of more-explosive eruptions in shallow water (surtseyan eruptions). Water depth also influenced the intermediate-depth erup-tion that occurred at SR in 1998–2001, with the emission of floating lava balloons (Kueppers et al. 2012).

The main morphometric parameters of the volcanic cones show values comparable to those of other submarine cones in Azores (e.g., Stretch et al. 2006; Tempera et al. 2013). The lack of significant correlations between different parameters suggests that the volcanic cones develop in a complex way and without self-similarity.

In summary, the results obtained have allowed us to enlarge the knowledge of volcanic and tectonic processes as well as their mutual interaction in a poorly studied geological setting, i.e., an ultra-slow oblique spreading axis. This study will un-derpin further detailed marine studies looking at the volcano-tectonic complexity of this area and, more generally, provides a useful comparison for similar submarine volcanic settings elsewhere.

Acknowledgments Data acquisition was conducted within the frame work of the project "Features of Azores and Italian Volcanic Islands (FAIVI)", supported by the European Commission 7th Framework Pro gramme under EUROFLEETS grant agreement no. 228344. The crews of the launch *Haliotis* and the R/V *L'Atalante* are gratefully acknowl edged for their assistance in data acquisition. We gratefully acknowledge J. White, A. Gudmundsson, N.C. Mitchell, D. Smith and an anonymous reviewer for their comments that improved the quality of the paper.

References

Andrew RE, Gudmundsson A (2007) Distribution, structure, and forma tion of Holocene lava shields in Iceland. J Volcanol Geotherm Res 168(1):137 154

Argus DF, Gordon RG, DeMets C, Stein S (1989) Closure of the Afric Eurasia North America plate motion circuit and tectonics of the Gloria fault. J Geophys Res 94:5585 5602

Babonneau N, Delacourt C, Cancouët R et al (2013) Direct sediment transfer from land to deep sea: insights into shallow multibeam ba thymetry at La Réunion Island. Mar Geol 346:47 57

Bacon CR, Duffield WA, Nakamura K (1980) Distribution of rhyolite domes of the Coso Range, California: implications for the extent of the geothermal anomaly. J Geophys Res 81:2425 2433

Beier C, Haase KM, Abouchami W, Krienitz M S, Hauff F (2008) Magma genesis by rifting of oceanic lithosphere above anomalous mantle: Terceira Rift, Azores. Geochem Geophys Geosyst 9: Q12013

Bonatti E, Harrison CGA (1988) Eruption styles of basalt in oceanic spreading ridges and seamounts: effect of magma temperature and viscosity. J Geophys Res 93:2967 2980

Booth B, Walker GPL, Croasdale R (1978) A quantitative study of five thousand years of volcanism on São Miguel, Azores. Philos Trans R Soc Lond, Ser A. 228:271 319

Borges JF, Bezzeghoud M, Buforn E, Pro C, Fitas A (2007) The 1980, 1997 and 1998 Azores earthquakes and some seismo tectonic im plications. Tectonophysics 435(1):37 54

Briais A, Sloan H, Parson LM, Murton BJ (2000) Accretionary processes in the axial valley of the Mid Atlantic Ridge 27° N 30° N from TOBI side scan sonar images. Mar Geophys Res 21(1 2):87 119

Buforn E, Udías A, Colombas MA (1988) Seismicity, source mechanisms and tectonics of the Azores Gibraltar plate boundary. Tectonophysics 152:89 118

Calais E, DeMets C, Nocquet JM (2003) Evidence for a post 3.16 Ma change in Nubia Eurasia North America plate motions? Earth Planet Sci Lett 216:81 92

Calvert AT, Moore RB, McGeehin JP, Rodrigues da Silva AM (2006) Volcanic history and 40Ar/39Ar and 14C geochronology of Terceira Island, Azores, Portugal. J Volcanol Geotherm Res 156:103 115

Cannat M, Briais A, Deplus C, Escartín J, Georgen JL, Mercouriev S, Meyzen C, Muller M, Pouliquen G, Rabain A, Silva P (1999) Mid AtlanticRidge Azores hotspot interactions: along axis migration of a hotspot derived event of enhanced magmatism 10 to 4 Ma ago. Earth Planet Sci Lett 173:257 269

Casalbore D, Romagnoli C, Bosman A, Chiocci FL (2011) Potential tsunamigenic landslides at Stromboli Volcano (Italy): Insight from marine DEM analysis. Geomorphology 126(1 2):42 50

Casalbore D, Bosman A, Romagnoli C, Chiocci FL (2014a) Large scale seafloor waveforms on the flanks of insular volcanoes (Aeolian Archipelago, Italy), with inferences about their origin. Mar Geol 355:318 329

Casalbore D, Bosman A, Romagnoli C, Chiocci, FL (2014b) Submarine mass movements on volcanic islands: examples from the Aeolian Archipelago (Italy). In Lollino G et al. (eds) Engineering Geology for Society and Territory Volume 4, Springer International Publishing, pp. 199 203

Casalbore D, Bosman A, Ridente D, Chiocci FL (2014c) Coastal and submarine landslides in the tectonically active Tyrrhenian Calabrian margin (Southern Italy): examples and geohazard impli cations In: Krastel et al (Eds) Submarine mass movements and their consequences, 6th International symposium, advances in natural and technological hazards research, 37:261 269

Casalbore D, Bosman A, Martorelli E, Sposato A, Chiocci FL (2014d) Mass wasting features on the submarine flanks of Ventotene volca nic edifice (Tyrrhenian Sea, Italy) In: Krastel et al (Eds) Submarine mass movements and their consequences, 6th International sympo sium, advances in natural and technological hazards research, 37: 285 293

Cashman KV, Fiske RS (1991) Fallout of pyroclastic debris from subma rine volcanic eruptions. Science 253:275 280

Chiocci FL, Romagnoli C, Casalbore D et al (2013) Bathy morphological setting of Terceira island (Azores) after the FAIVI cruise. J Maps 9: 590 595

Clague DA, Moore JG, Reynolds JR (2000) Formation of submarine flat topped volcanic cones in Hawai'i. Bull Volcanol 62(3):214 233

Clark RM, Cox SJD (1996) A modern regression approach to determin ing fault displacement scaling relationships. J Struct Geol 18:147 152

Colman A et al (2012) Effects of variable magma supply on mid ocean ridge eruptions: constraints from mapped lava flow fields along the Galapagos Spreading Center. Geochem Geophys Geosyst 13, Q08014. doi:10.1029/ 2012GC004163

Coltelli M, D'Anna G, Cavallaro D, et al. (2012) Ferdinandea 2012: the oceanographic cruise on the graham bank, Strait of Sicily. In pro ceeding of GNGTS 2012, 207 212

Costa ACG, Marques FO, Hildenbrand A, Sibrant ALR, Catita CMS (2014) Large scale catastrophic flank collapses in a steep volcanic ridge: the Pico Faial Ridge, Azores Triple Junction. J Volcanol Geotherm Res 272:111 125

DeMets C, Gordon RG, Argus DF (2010) Geologically current plate motions. Geophys J Int 181:1 80

Dias NA, Matias L, Lourenço N, Madeira J, Carrilho F, Gaspar JL (2007) Crustal seismic velocity structure near Faial and Pico islands (AZORES), from local earthquake tomography. Tectonophysics 445:301 317

Edwards MH, Kurras GJ, Tolstoy M, Bohnenstiehl DR, Coakley BJ, Cochran JR (2001) Evidence of recent volcanic activity on the ultraslow spreading Gakkel ridge. Nature 409(6822):808 812

Instituto Geográfico do Exército (2002a) Angra do Heroísmo (Terceira Açores) Folha 24, Carta Militar de Portugal Série M889, 2nd ed. Instituto Geográfico do Exército, Lisboa

Instituto Geográfico do Exército (2002b) Biscoitos (Terceira Açores) Folha 22, Carta Militar de Portugal Série M889, 2nd ed. Instituto Geográfico do Exército, Lisboa

Instituto Geográfico do Exército (2002c) Praia da Vitória (Terceira Açores) Folha 23 Carta Militar de Portugal Série M889, 2nd ed. Instituto Geográfico do Exército, Lisboa

Instituto Geográfico do Exército, (2002d) Ribeirinha (Terceira Açores) Folha 25 Carta Militar de Portugal Série M889, 2nd ed. Instituto Geográfico do Exército, Lisboa

Favalli M, Karátson D, Mazzarini F, Pareschi MT, Boschi E (2009) Morphometry of scoria cones located on a volcano flank: a case study from Mt. Etna (Italy), based on high resolution LiDAR data. J Volcanol Geotherm Res 186(3):320 330

Fisher R (1984) Submarine volcaniclastic rocks. Geol Soc Lond Spec Publ 16(1):5 27

Gente P, Dyment J, Maia M, Goslin J (2003) Interaction between the Mid Atlantic Ridge and the Azores hot spot during the last 85 Myr: emplacement and rifting of the hot spot derived plateaus.

Geochem Geophys Geosyst 4(10):8514. doi:10.1029/2003GC00052
Gertisser R, Self S, Gaspar JL, Kelley SP, Pimentel A, Eikenberg J, Barry TL, Pacheco JM, Queiroz G, Vespa M (2010) Ignimbrite stratigra phy and chronology on Terceira Island, Azores. Geol Soc Am S 464: 133 154
Gudmundsson A (1986) Mechanical aspects of postglacial volcanism and tectonics of the Reykjanes Peninsula, southwest Iceland. J Geophys Res 91(B12):12711 12721
Gudmundsson A (2000) Fracture dimensions, displacements and fluid transport. Journal Struct Geol 22:1221 1231
Gudmundsson A (2005) Effects of mechanical layering on the develop ment of normal faults and dykes in Iceland. Geodin Acta 18:11 30
Gudmundsson A (2007) Infrastructure and evolution of ocean ridge dis continuities in Iceland. J Geodynamics 43(1):6 29
Gudmundsson A, De Guidi G, Scudero S (2013) Length displacement scaling and fault growth. Tectonophysics 608:1298 1309
Head JW, Wilson L, Smith DK (1996) Mid ocean ridge eruptive vent morphology and substructure: evidence for the dike widths, eruption rates, and axial volcanic ridges. J Geophysic Res 101:28265 28280
Hildenbrand A, Madureira P, Marques FO, Cruz I, Henry B, Silva P (2008) Multi stage evolution of a sub aerial volcanic ridge over the last 1.3 Myr: S. Jorge Island, Azores Triple Junction. Earth Planet Sci Lett 273:289 298
Hildenbrand A, Marques FO, Catalão J, Catita CMS, Costa ACG (2012) Large scale active slump of the southeastern flank of Pico Island, Azores. Geology 40:939 942
Hildenbrand A, Weis D, Madureira P, Marques FO (2014) Recent plate re organization at the Azores Triple Junction: evidence from com bined geochemical and geochronological data on Faial, S. Jorge and Terceira volcanic islands. Lithos 210:27 39
Hipólito A, Madeira J, Carmo R, Gaspar JL (2013) Neotectonics of Graciosa Island (Azores): a contribution to seismic hazard assess ment of a volcanic area in a complex geodynamic setting. Ann Geophys 56(6):S0677. doi:10.4401/ag 6222
Hirn A, Haessler H, Hoang Tronc P, Wittlinger G, Mendes VL (1980) Aftershock sequence of the January 1, 1980 earthquake and present day tectonics in the Azores. Geophys Res Lett 7:501 504
Höskuldsson Á, Hey R, Kjartansson E, Guðmundsson GB (2007) The Reykjanes Ridge between 63 10′ N and Iceland. J Geodynamics 43(1):73 86
Kelly JT, Carey S, Pistolesi M, Rosi M, Croff Bell KL, Roman C, Marani M (2014) Exploration of the 1891 Foerstner submarine vent site (Pantelleria, Italy): insights into the formation of basaltic balloons. Bull Volcanol 76(7):1 18
Kokelaar BP, Durant GP (1983) The submarine eruption and erosion of Surtla (Surtsey), Iceland. J Volcanol Geotherm Res 19:239 246
Kueppers U, Nichols AR, Zanon V, Potuzak M, Pacheco JM (2012) Lava balloons peculiar products of basaltic submarine eruptions. Bull Volcanol 74(6):1379 1393
Leat PT, Tate AJ, Tappin DR, Day SJ, Owen MJ (2010) Growth and mass wasting of volcanic centers in the northern South Sandwich arc, South Atlantic, revealed by new multibeam mapping. Mar Geol 275(1):110 126
Ligi M, Mitchell NC, Marani M, Gamberi F, Pentitenti D, Carrara G, Rovere M, Portaro R, Centorami G, Bortoluzzi G, Jacobs C, Rouse I, Flewellen C, Whittle S, Terrinha P, Freire Luis J, Lourenço N (1999) Giant volcanic ridges amongst the Azores Islands. Presented at Fall meeting of the American Geophysical Union
Lockwood JP, Dvorak JJ, English TT, Koyanagi RY, Okamura AT, Summers ML, Tanigawa WR (1987) Mauna Loa 1974 1984: a decade of intrusive and extrusive activity. US Geol Surv Prof Pap 1350:537 570
Lourenço (2007) Tectono Magmatic processes at the Azores Triple Junction. Unpublished PhD dissertation
Lourenço N, Miranda J, Luis J, Ribeiro A, Mendes Victor L, Madeira J, Needham H (1998) Morpho tectonic analysis of the Azores Volcanic Plateau from a new bathymetric compilation of the area. Mar Geophys Res 20:141 156
Luís JF, Miranda JM (2008) Reevaluation of magnetic chrons in the North Atlantic between 35°N and 47°N: implications for the forma tion of the Azores Triple Junction and associated plateau. J Geophys Res 113, B1o1o5. doi:10.1029/2007Jb005573
Luís JF, Miranda JM, Galdeano A, Patriat P (1998) Constraints on the structure of the Azores spreading center from gravity data. Mar Geophys Res 20:157 170
Machado F (1959) Submarine pits of the Azores Plateau. Bull Volcanol TXXI 109 116
Madeira J (2005) The volcanoes of Azores island: a world class heritage (examples from Terceira, Pico and Faial Islands), IV Internacional Symposium ProGEO on the Conservation of the Geological Heritage Field Trip Book. European Association for the Conservation of the Geological Heritage and Centro de Geociências da Universidade do Minho, Braga
Madeira J, Brum da Silveira A (2003) Active tectonics and first paleoseismological results in Faial, Pico and S. Jorge islands (Azores, Portugal). Ann Geophys 46:733 761
Madeira J, Ribeiro A (1990) Geodynamic models for the Azores triple junction: a contribution from tectonics. Tectonophysics 184:405 415
Masson DG, Watts AB, Gee MJR, Urgeles R, Mitchell NC, Le Bas TP, Canals M (2002) Slope failures on the flanks of the western Canary Islands. Earth Sci Rev 57:1 35
McClinton T, White SM, Colman A, Sinton JM (2013) Reconstructing lava flow emplacement processes at the hot spot-affected Galápagos Spreading Center, 95° W and 92° W. Geochem Geophys Geosyst 14(8):2731 2756
Mendes VB, Madeira J, Brum da Silveira A, Trota A, Elósegui P, Pagarete J (2013) Present day deformation in São Jorge Island, Azores, from episodic GPS measurements (2001 2011). Adv Space Res 51:1581 1592
Miranda JM, Luis JF, Abreu I, Mendes Victor LA, Galdeano A, Rossignol JC (1991) Tectonic framework of the Azores triple junc tion. Geophys Res Lett 188:1421 1424
Miranda JM, Victor LAM, Simoes JZ et al (1998) Tectonic setting of the Azores Plateau deduced from an OBS survey. Mar Geophys Res 20: 171 182
Miranda JM, Navarro A, Catalão J, Fernandes RMS (2012) Surface dis placement field at Terceira island deduced from repeated GPS mea surements. J Volcanol Geotherm Res 217 218:1 7
Mitchell NC (2003) Susceptibility of mid ocean ridge volcanic islands and seamounts to large scale landsliding. J Geophys Res 108(B8): 2397
Mitchell NC, Beir C, Rosin PL, Quartau R, Tempera F (2008) Lava penetrating water: submarine lava flows around the coasts of Pico Island, Azores. Geochem Geophys Geosyst 9:Q03024. doi:10.1029/ 2007GC001725
Mitchell NC, Stretch R, Oppenheimer C, Kay D, Beier C (2012a) Cone morphologies associated with shallow marine eruptions: east Pico Island, Azores. Bull Volcanol 74(10):2289 2301
Mitchell NC, Quartau R, Madeira J (2012b) Assessing landslide move ments in volcanic islands using near shore marine geophysical data: south Pico island, Azores. Bull Volcanol 74(2):483 496
Montanaro C, Beget J (2011) Volcano collapse along the Aleutian Ridge (western Aleutian Arc). 734 Nat Haz Earth Sys Sci 11:715 730
Moore JG, Normark WR, Holcomb RT (1994) Giant Hawaiian land slides. Annu Rev Earth Planet Sci 22:119 144
Oehler JF, Lénat JF, Labazuy P (2008) Growth and collapse of the Reunion Island volcanoes. Bull Volcanol 70:717 742

Parson LM, Murton BJ, Searle RC et al (1993) En echelon volcanic ridges at the Reykjanes Ridge: a life cycle of volcanism and tecton ics. Earth Planet Sci Lett 117:73 87

Pascoal A, Silvestre C, Oliveira P (2006) Vehicle and mission control of single and multiple autonomous marine robots. In: Roberts GN, Sutton R (eds) Advances in unmanned marine vehicles. IET, London, pp 353 380

Paull CK, Ussler W III, Caress DW et al (2010) Origins of large crescent shaped bedforms within the axial channel of Monterey Canyon. Geosphere 6:755 774

Porter SC (1972) Distribution, morphology, and size frequency of cinder cones on Mauna Kea volcano, Hawaii. Geol Soc Am Bull 83:3607 3612

Quartau R, Trenhaile AS, Mitchell NC, Tempera F (2010) Development of volcanic insular shelves: Insights from observations and model ling of Faial Island in the Azores Archipelago. Mar Geol 275:66 83

Quartau R, Tempera F, Mitchell NC, Pinheiro LM, Duarte H, Brito PO, Bates R, Monteiro JH (2012) Morphology of the Faial Island shelf (Azores): the interplay between volcanic, erosional, depositional, tectonic and mass wasting processes. Geochem Geophys Geosy 13, Q04012

Quartau R, Hipólito A, Romagnoli C, Casalbore D, Madeira J, Tempera F, Roque C, Chiocci FL (2014) The morphology of insular shelves as a key for understanding the geological evolution of volcanic islands: insights from Terceira Island (Azores). Geochem Geophys Geosy 15:1801 1826

Romagnoli C, Casalbore D, Chiocci FL, Bosman A (2009a) Offshore evidence of large scale lateral collapses on the eastern flank of Stromboli, Italy, due to structurally controlled, bilateral flank insta bility. Mar Geol 262:1 13

Romagnoli C, Kokelaar P, Casalbore D, Chiocci FL (2009b) Lateral collapses and active sedimentary processes on the northwestern flank of Stromboli volcano, Italy. Mar Geol 265:101 119

Romagnoli C, Casalbore D, Chiocci FL (2012) La Fossa caldera breaching and submarine erosion (Vulcano island, Italy). Mar Geol 303 306:87 98

Romagnoli C, Casalbore D, Bosman A, Braga R, Chiocci FL (2013) Submarine structure of Vulcano Volcano (Aeolian Islands) revealed by high resolution bathymetry and seismo acoustic data. Mar Geol 338:30 45

Ryan WBF, Carbotte SM, Coplan JO et al (2009) Global multi resolution topography synthesis. Geochem Geophys Geosyst 10, Q03014

Sauter D, Parson L, Mendel V, Rommevaux Jestin C, Gomez O, Briais A, Mevel C, Tamaki K, the FUJI Scientific Team (2002) TOBI sidescan sonar imagery of the very slow spreading Southwest Indian Ridge: evidence for along axis magma distribution. Earth Planet Sci Lett 199(1 2):81 95

Schlische RW, Young SS, Ackermann RV, Gupta A (1996) Geometry and scaling relations of a population of very small rift related normal faults. Geology 24:683 686

Searle RC, Keeton JA, Lee SM, Owens R, Mecklenburgh R, Parsons B, White RS (1998) The Reykjanes Ridge: structure and tectonics of a hot spot influenced, slow spreading ridge, from multibeam bathy metric, gravity and magnetic investigations. Earth Planet Sci Lett 160:463 478

Searle RC, Murton BJ, Achenbach K et al (2010) Structure and develop ment of an axial volcanic ridge: Mid Atlantic Ridge, 45 N. Earth Planet Sci Lett 299(1):228 241

Self S (1976) The recent volcanology of Terceira, Azores. J Geol Soc Lond 132:645 666

Settle M (1979) The structure and emplacement of cinder cone fields. Am J Sci 279:1089 1107

Silva R, Havskov J, Bean C, Wallenstein N (2012) Seismic swarms, fault plane solutions, and stress tensors for São Miguel Island central region (Azores). J Seismol 16:389 407

Smith DK, Cann JR (1993) Building the crust at the Mid Atlantic Ridge. Nature 365(6448):707 715

Smith DK, Cann JR (1999) Constructing the upper crust of the Mid Atlantic Ridge: a reinterpretation based on the Puna Ridge, Kilauea Volcano. J Geophys Res 104:25379 25399

Smith DK, Tivey MA, Gregg PM, Kong LSL (2001) Magnetic anomalies at the Puna Ridge, a submarine extension of Kilauea Volcano: implications for lava deposition. J Geophys Res 106(B8):16047 16060

Stretch R, Mitchell NC, Portaro RA (2006) A morphometric analysis of the submarine volcanic ridge of Pico Island. J Volcanol Geotherm Res 156:35 54

Tempera F, Hipolito A, Madeira J, Vieira S, Campos A, Mitchell NC (2013) Condor seamount (Azores, NE Atlantic): a morpho tectonic interpretation. Deep Sea Res Part II Top Stud Oceanogr 98:7 23

Tibaldi A, Lagmay AMF (2006) Interaction between volcanoes and their basement. J Volcanol Geotherm Res 158(1):1 5

Trippanera D, Porreca M, Ruch J, Pimentel A, Acocella V, Pacheco J, Salvatore M (2014) Relationships between tectonics and magmatism in a transtensive/transform setting: an example from Faial Island (Azores, Portugal). Geol Soc Am Bull 126(1 2):164 181

Vogt PR, Jung WY (2004) The Terceira Rift as hyper slow, hotspot dominated oblique spreading axis: a comparison with other slow spreading plate boundaries. Earth Planet Sci Lett 218: 77 90

Walker GPL (1999) Volcanic rift zones and their intrusions swarms. J Volcanol Geother Res 94:21 34

Weston FS (1964) List of recorded volcanic eruptions in the Azores with brief reports. Bol Mus Lab Min Geol Fac Ciên Lisboa 10:3 18

Zanon V, Pimentel A (2015) Spatio temporal constraints on magma stor age and ascent conditions in a transtensional tectonic setting: the case of the Terceira Island (Azores). Am Mineral. doi:10.2138/am 2015 4936